

Parity violating Møller scattering asymmetry up to the two-loop level

A. G. Aleksejevs

*Memorial University, Corner Brook, Canada**

S. G. Barkanova

Acadia University, Wolfville, Canada†

Yu. M. Bystritskiy and E. A. Kuraev

Joint Institute for Nuclear Research, Dubna, Russia‡

A. N. Ilyichev

National Center of Particle and High Energy Physics of Belarussian State University, Minsk, Belarus§

V. A. Zykunov

Belarusian State University of Transport, Gomel, Belarus¶

(Dated: October 16, 2018)

The paper investigates contributions of Z , W and γ intermediate states to the parity-violating Møller scattering asymmetry up to two-loop level. Using the Yennie–Frautschi–Suura factorization form for amplitudes, we demonstrate that QED corrections, with an exception of vacuum-polarization effects, cancel at the asymmetry level. We obtain chiral amplitudes at Born, one-loop and partially at two-loop level: boxes with lepton self-energies, ladder boxes and decorated boxes. Our calculations are relevant for the ultra-precise 11 GeV MOLLER experiment planned at Jefferson Laboratory and future ILC experiments. The numerical comparison of the two-loop contributions with the experimental accuracy of MOLLER is provided.

I. INTRODUCTION

The Standard Model of Particle Physics (SM) introduces a non-zero asymmetry between left- and right-handed particles and predicts a parity-violating (PV) interference between the electromagnetic and weak neutral current amplitudes. By measuring this small asymmetry, precision experiments with polarized electron beams (polarized Møller scattering) attract especially active interest from both experimental and theoretical communities as they can provide indirect access to physics at multi-TeV scales and play an important complementary role to the LHC research program.

The MOLLER (Measurement Of a Lepton Lepton Electroweak Reaction) experiment planned at Jefferson Lab aims to measure the parity-violating asymmetry in the scattering of 11 GeV longitudinally-polarized electrons from the atomic electrons in a liquid hydrogen target (Møller scattering) with a combined statistical and systematic uncertainty of 2% [1–4]. At such precision, any inconsistency with the SM predictions will clearly signal new physics. However, a comprehensive analysis of radiative corrections is needed before any conclusions can be made. Since MOLLER’s stated precision goal is significantly more ambitious than that of its predecessor E-158 [5–7], theoretical input for this measurement must include not only a full treatment of one-loop (next-to-leading order, NLO) electroweak radiative corrections but also leading two-loop corrections (next-to-next-leading order, NNLO). A significant theoretical effort has been dedicated to the one-loop radiative corrections already [8–15] (the squares of the one-loop diagrams were calculated in [16]), but more needs to be done on the two-loop corrections.

The main goal of this paper is to verify the previous theoretical predictions for the Møller asymmetry using the Yennie–Frautschi–Suura factorization technique, and to obtain an estimation of some leading two-loop corrections: boxes with lepton self-energies, ladder (double) boxes, and decorated boxes. We show that at the next-to-leading order, the main contribution to the Møller asymmetry comes from the process with Z and W gauge bosons in the intermediate state and most of the pure-QED contributions cancel out. Using the hypothesis of factorization of soft

*Electronic address: aaleksejevs@grenfell.mun.ca

†Electronic address: svetlana.barkanova@acadiau.ca

‡Electronic address: bystr@theor.jinr.ru

§Electronic address: ily@hep.by

¶Electronic address: vladimir.zykunov@cern.ch

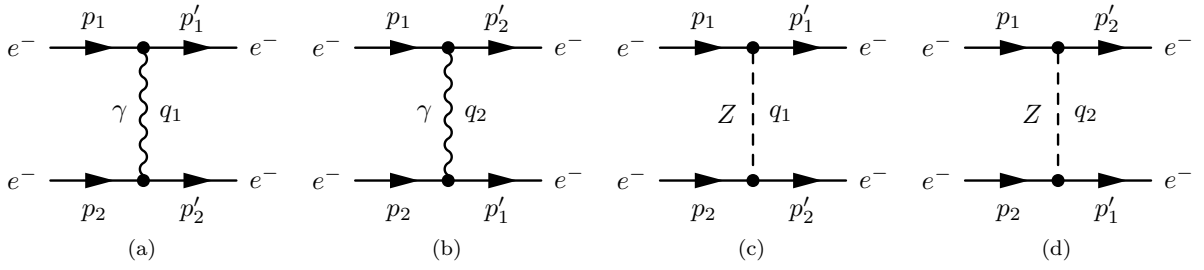


Figure 1: Born approximation diagrams.

and hard contributions, similar to that of the Drell–Yan parton picture, we calculate the SM electroweak corrections at the NLO and partially at the next-to-NLO levels. Detailed and consistent consideration of all two-loop corrections will be the next task of our group: these are the combined self-energy (SE) and vertex contributions, double SEs, decorated and double vertices, and boxes with vertex and SE insertions. Our calculations are performed using a one-mass shell renormalization scheme in the t’Hooft–Feynman gauge.

The paper is organized as follows. In Section II, we state the PV Møller scattering asymmetry in the Born approximation. Section III briefly discusses approximations we use in calculating the electroweak radiative corrections. Section IV outlines our treatment of infrared-divergent contributions. The Yennie–Frautschi–Suura (YFS) irreducible diagrams are evaluated in Section V. One-loop and some two-loop radiative corrections are given in Sections VI and VII, correspondingly. The results are gathered and analyzed in Section VIII, and are followed by conclusions in Section IX. Details and examples of our calculations are given in the Appendices.

II. ASYMMETRY IN THE BORN APPROXIMATION

The Møller process first studied by [17] is the process of electron–electron scattering defined as follows:

$$e^-(p_1, \lambda_1) + e^-(p_2, \lambda_2) \rightarrow e^-(p'_1, \lambda'_1) + e^-(p'_2, \lambda'_2). \quad (1)$$

The amplitude (matrix element) of this process within the SM has four terms (see Fig. 1):

$$\mathcal{M}^{(0)} = \mathcal{M}_{\gamma_1}^{(0)} - \mathcal{M}_{\gamma_2}^{(0)} + \mathcal{M}_{Z_1}^{(0)} - \mathcal{M}_{Z_2}^{(0)}, \quad (2)$$

where $\mathcal{M}_{\gamma_1}^{(0)}$ is the contribution from a photon exchange in the t -channel (Fig. 1(a)) and $\mathcal{M}_{\gamma_2}^{(0)}$ is the contribution from a photon exchange in the u -channel, where the two final leptons are interchanged ($p'_1 \leftrightarrow p'_2$) to accommodate the Pauli principle (see Fig. 1(b)). The last two terms, $\mathcal{M}_{Z_{(1,2)}}^{(0)}$ are similar contributions with a Z boson exchange in the t - and u -channels (see Fig. 1(c),1(d)). Using the t’Hooft–Feynman gauge, i.e. $\xi = 1$, we get the following form for these terms:

$$\begin{aligned} \mathcal{M}_{\gamma_1}^{(0)} &= \frac{e^2}{q_1^2} \left[\bar{u}^{(\lambda'_1)}(p'_1) \gamma^\mu u^{(\lambda_1)}(p_1) \right] \left[\bar{u}^{(\lambda'_2)}(p'_2) \gamma_\mu u^{(\lambda_2)}(p_2) \right], \\ \mathcal{M}_{\gamma_2}^{(0)} &= \frac{e^2}{q_2^2} \left[\bar{u}^{(\lambda'_2)}(p'_2) \gamma^\mu u^{(\lambda_1)}(p_1) \right] \left[\bar{u}^{(\lambda'_1)}(p'_1) \gamma_\mu u^{(\lambda_2)}(p_2) \right], \\ \mathcal{M}_{Z_1}^{(0)} &= \frac{g^2}{16 \cos^2 \theta_W} \left[\bar{u}^{(\lambda'_1)}(p'_1) \gamma_\mu (a - \gamma_5) u^{(\lambda_1)}(p_1) \right] \left[\bar{u}^{(\lambda'_2)}(p'_2) \gamma^\mu (a_V - \gamma_5) u^{(\lambda_2)}(p_2) \right] \frac{1}{q_1^2 - M_Z^2}, \\ \mathcal{M}_{Z_2}^{(0)} &= \frac{g^2}{16 \cos^2 \theta_W} \left[\bar{u}^{(\lambda'_2)}(p'_2) \gamma_\mu (a - \gamma_5) u^{(\lambda_1)}(p_1) \right] \left[\bar{u}^{(\lambda'_1)}(p'_1) \gamma^\mu (a_V - \gamma_5) u^{(\lambda_2)}(p_2) \right] \frac{1}{q_2^2 - M_Z^2}, \end{aligned}$$

where $q_1 = p_1 - p'_1 = p'_2 - p_2$ and $q_2 = p_1 - p'_2 = p'_1 - p_2$ are the transferred momenta in the direct and exchanged diagrams, $a_V = 1 - 4 \sin^2 \theta_W$, θ_W is the Weinberg angle ($g \sin \theta_W = e$), and e is the electric charge of a positron.

In the chiral amplitude approach we are using, the specific chiral spin states of the initial and final particles are selected as

$$u^{(\lambda)} = \omega_\lambda u, \quad \bar{u}^{(\lambda)} = \bar{u} \omega_{-\lambda}, \quad \lambda = \pm 1 = R, L, \quad (3)$$

where chirality projection operators ω_λ have the following form:

$$\omega_\lambda = \frac{1}{2}(1 + \lambda\gamma_5), \quad \omega_\lambda^2 = \omega_\lambda, \quad \omega_+\omega_- = 0, \quad \omega_+ + \omega_- = 1. \quad (4)$$

For the case of massless fermions, we need to satisfy the completeness condition:

$$u^{(\lambda)}(p)\bar{u}^{(\lambda)}(p) = \omega_\lambda\hat{p}. \quad (5)$$

Let us calculate the QED contribution of a right+right \rightarrow right+right ($++ \rightarrow ++$) chiral amplitude, where all fermions are right-handed, i.e. $u^R = \omega_+u$:

$$\begin{aligned} \mathcal{M}_{\gamma_1}^{(0)++++} &= \frac{e^2}{t} [\bar{u}(p'_1)\omega_-\gamma^\mu\omega_+u(p_1)] [\bar{u}(p'_2)\omega_-\gamma_\mu\omega_+u(p_2)], \\ \mathcal{M}_{\gamma_2}^{(0)++++} &= \frac{e^2}{u} [\bar{u}(p'_2)\omega_-\gamma^\mu\omega_+u(p_1)] [\bar{u}(p'_1)\omega_-\gamma_\mu\omega_+u(p_2)]. \end{aligned}$$

Here, we have used the Mandelstam invariants in the limit of vanishing electron mass ($m \rightarrow 0$):

$$s = 2(p_1p_2) = 2(p'_1p'_2), \quad t = -2(p_1p'_1) = -2(p_2p'_2), \quad u = -2(p_1p'_2) = -2(p_2p'_1), \quad s + t + u = 0. \quad (6)$$

In order to transform these amplitudes into calculable traces, we multiply terms which contain a factor $1/t$ by the following quantity:

$$\frac{ab}{ab} = 1, \quad (7)$$

and the terms with factor $1/u$ by

$$\frac{cd}{cd} = 1, \quad (8)$$

where

$$\begin{aligned} a &= \bar{u}(p_1)\omega_-\hat{p}_2\omega_+u(p'_2), & c &= \bar{u}(p_1)\omega_-\hat{p}_2\omega_+u(p'_1), \\ b &= \bar{u}(p_2)\omega_-\hat{p}_1\omega_+u(p'_1), & d &= \bar{u}(p_2)\omega_-\hat{p}_1\omega_+u(p'_2). \end{aligned} \quad (9)$$

This allows us to obtain the trace in the numerator and calculate it immediately:

$$\begin{aligned} \mathcal{M}_{\gamma_1}^{(0)++++} &= \frac{e^2}{t} \frac{1}{ab} \text{Sp} [\hat{p}'_1\gamma_\mu\omega_+\hat{p}_1\hat{p}_2\omega_+\hat{p}'_2\gamma^\mu\omega_+\hat{p}_2\hat{p}_1\omega_+] = \frac{e^2}{t} \frac{1}{ab} 2s^2t, \\ \mathcal{M}_{\gamma_2}^{(0)++++} &= \frac{e^2}{u} \frac{1}{cd} \text{Sp} [\hat{p}'_2\gamma_\mu\omega_+\hat{p}_1\hat{p}_2\omega_+\hat{p}'_1\gamma^\mu\omega_+\hat{p}_2\hat{p}_1\omega_+] = \frac{e^2}{u} \frac{1}{cd} 2s^2u. \end{aligned} \quad (10)$$

Thus, the QED amplitude in the Born approximation has the form

$$\mathcal{M}_\gamma^{(0)++++} = \mathcal{M}_{\gamma_1}^{(0)++++} - \mathcal{M}_{\gamma_2}^{(0)++++} = 2(4\pi\alpha)s^2\mathcal{M}_\gamma^0, \quad \mathcal{M}_\gamma^0 = \frac{1}{ab} - \frac{1}{cd}. \quad (11)$$

The rest of the spiral amplitudes are calculated in a similar way and lead to the following results:

$$\begin{aligned} \mathcal{M}_\gamma^{(0)++--} &= 2(4\pi\alpha)\frac{u^2}{tc_1d_1}, \\ \mathcal{M}_\gamma^{(0)+++-} &= -2(4\pi\alpha)\frac{t^2}{uc_1d_1}, \end{aligned} \quad (12)$$

where c_1 and d_1 are the modified factors similar to (7) or (8), which in this case have the form:

$$c_1 = \bar{u}(p_1)\omega_-(p'_2), \quad d_1 = \bar{u}(p_2)\omega_+u(p'_1). \quad (13)$$

Using relations

$$|a|^2 = |b|^2 = -st, \quad |c|^2 = |d|^2 = -su, \quad abc^*d^* = -s^2tu, \quad (14)$$

we obtain the well-known result [18, 19] for the sum of squares of all six amplitudes:

$$\sum_{(\lambda)} \left| \mathcal{M}_{\gamma}^{(0)\lambda} \right|^2 = 8(4\pi\alpha)^2 \left[\left(\frac{s^2}{t^2} + \frac{s^2}{u^2} + \frac{2s^2}{tu} \right) + \left(\frac{t^2}{u^2} + \frac{u^2}{t^2} \right) \right] = 8(4\pi\alpha)^2 \frac{s^4 + t^4 + u^4}{t^2 u^2}. \quad (15)$$

Employing the same procedure for the amplitudes with a mediating Z boson, we obtain

$$\mathcal{M}_Z^{(0)++++} = \mathcal{M}_{Z_1}^{(0)++++} - \mathcal{M}_{Z_2}^{(0)++++} = -\frac{2s^2}{M_Z^2} \frac{4\pi\alpha}{4\sin^2(2\theta_W)} (1 + a_V)^2 \mathcal{M}_Z^0, \quad \mathcal{M}_Z^0 = \frac{t}{ab} - \frac{u}{cd}. \quad (16)$$

The expressions for the amplitude \mathcal{M}_Z^{----} can be obtained from (11) and (16) by replacing the factor $(a_V + 1)^2$ with $(a_V - 1)^2$.

The high-precision Møller scattering experiments allow a careful study of the SM predictions by measuring the polarization asymmetry defined in the standard way as

$$A \equiv A_{LR} = \frac{\sigma_{LL} + \sigma_{LR} - \sigma_{RL} - \sigma_{RR}}{\sigma_{LL} + \sigma_{LR} + \sigma_{RL} + \sigma_{RR}} = \frac{\sigma_{LL} - \sigma_{RR}}{\sigma_{00}}, \quad (17)$$

where σ means the differential cross section ($\sigma \equiv d\sigma/dc$), $c = \cos(\widehat{\mathbf{p}_1, \mathbf{p}'_1})$, and the index 00 corresponds to unpolarized scattering. Using the language of chiral amplitudes, this asymmetry reads as

$$A = \frac{\sigma^{----} - \sigma^{++++}}{\sigma^{++++} + \sigma^{+--+} + \sigma^{+-+-} + \sigma^{-+-+} + \sigma^{-+--} + \sigma^{----}}. \quad (18)$$

In the Born approximation, the only contribution to this asymmetry comes from an interference between $\mathcal{M}_{\gamma}^{(0)}$ and $\mathcal{M}_Z^{(0)}$, which is proportional to

$$(\mathcal{M}_{\gamma}^0)^* \mathcal{M}_Z^0 = \left(\frac{1}{ab} - \frac{1}{cd} \right)^* \left(\frac{t}{ab} - \frac{u}{cd} \right) = -\frac{2}{stu}. \quad (19)$$

This gives us the following expression for the Born asymmetry:

$$A^{(0)} = \frac{s}{2M_W^2} A_0 \frac{1 - 4\sin^2\theta_W}{\sin^2\theta_W}, \quad A_0 = \frac{y(1-y)}{1+y^4+(1-y)^4}, \quad y = \frac{-t}{s} = \frac{1-c}{2}. \quad (20)$$

In spite of this asymmetry being extremely small ($\sim 10^{-7}$), the accuracy of modern and upcoming experiments clearly exceeds the accuracy of the theoretical result in the Born approximation. In addition, one-loop contributions to the parity-violating Møller scattering asymmetry were found to be very large [10, 11, 14], which points to the extreme importance of the careful inclusion of the higher-order radiative corrections.

III. GENERAL DISCUSSION OF RADIATIVE CORRECTIONS

Radiative corrections are the higher-order contributions to the leading-order Feynman diagrams, and their inclusion is an essential part of any modern experiment. In this work, we consider the SM and QED radiative corrections at the one- and two-loop levels. Although some progress [14, 16] has recently been achieved in calculating radiative corrections for Møller scattering with semi-automated computer-algebra packages like FeynArts [20], FormCalc [21], LoopTools [21] and Form [22], we believe that since work on the two-loop corrections is still at an early stage, it is prudent to do careful and explicit derivations first, with semi-automated results to follow later.

Obviously, at this stage some approximations are unavoidable. A helpful approximation we employ throughout this work is based on the effective factorization of contributions from the emission of real soft photons and virtual photons with small virtuality [23]. In this approximation, we can omit all Feynman diagrams with virtual photons connecting external (on-mass-shell) electron lines. The same statement is valid for the emission of real soft photons. This approximation significantly reduces the number of diagrams we have to evaluate. The relevant modification of the Born asymmetry A is discussed in Section V. Another simplification we use is neglecting the dependence on the external momenta.

In addition to bremsstrahlung, the types of Feynman amplitudes we consider at one-loop level are vacuum polarization diagrams (Fig. 3), boxes (Fig. 4), and vertex corrections (Fig. 5). At the two-loop level, we evaluate the self-energy insertions into lepton lines in the two-boson exchange boxes and the two types of the double-box diagrams – ladder type and decorated-box type. The following contributions from SM corrections are to be considered later: the boxes with 1) vertices and 2) SE insertions, 3) combined SE and vertex contributions, 4) double SEs, 5) decorated and 6) double vertices.

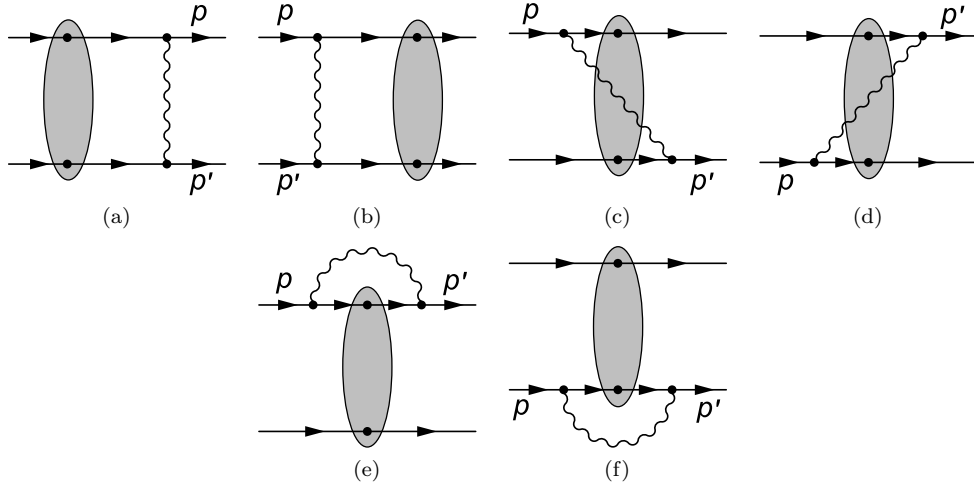


Figure 2: Demonstration of YFS irreducible hard subprocess in first order of perturbation theory (see for details Section IV).

IV. EXTRACTION OF THE INFRARED-DIVERGENT PART

A comprehensive and detailed analysis of infrared-divergent contributions for a general case was performed by [23]. Following the [23] findings, we express contributions from infrared-divergent radiative corrections in the form of an exponent convoluted with the infrared-finite hard subprocess part of the amplitude.

Let us review some of the [23] results which we use in this work. The amplitude of any process with external (ingoing and outgoing) charged particles has the form:

$$\mathcal{M}(p, p') = \sum_{n=0}^{\infty} \mathcal{M}_n, \quad (21)$$

where p and p' are the external on-mass shell particle momenta (see for, example, Fig. 2 notation), a summation is done over different orders of perturbation theory contributions coming from the emission of n virtual photons, and \mathcal{M}_n is the amplitude of the process in the n -th order of perturbation (i.e. proportional to e^n , where e is the positron charge).

It has been proven that the amplitudes \mathcal{M}_n have the following structure:

$$\begin{aligned} \mathcal{M}_0 &= m_0, \\ \mathcal{M}_1 &= \alpha B m_0 + m_1, \\ \mathcal{M}_2 &= \frac{(\alpha B)^2}{2!} m_0 + \alpha B m_1 + m_2, \\ &\dots \\ \mathcal{M}_n &= \sum_{r=0}^n \frac{(\alpha B)^r}{r!} m_{n-r}, \end{aligned} \quad (22)$$

where m_0 is the amplitude in the Born approximation and m_n ($n > 0$) are the infrared-finite pieces of the amplitude of n -th order in the perturbation theory (we call it *hard subprocess amplitude*). Fig. 2 illustrates the amplitude m_1 with the hard subprocess showed by filled blocks. The term B introduced in (22) has the form:

$$B = \frac{i}{(2\pi)^3} \int \frac{d^4 k}{k^2 - \lambda^2} \left(\frac{2p'_\mu - k_\mu}{2(p'k) - k^2} - \frac{2p_\mu - k_\mu}{2(pk) - k^2} \right)^2, \quad (23)$$

where k and λ are the momentum and the photon mass parameter, which we will take to the zero limit later. Thus using the structure of the n -th order amplitude defined by (22), for the total amplitude we can write:

$$\mathcal{M} = \sum_{n=0}^{\infty} \sum_{r=0}^n \frac{(\alpha B)^r}{r!} m_{n-r} = \sum_{r=0}^{\infty} \frac{(\alpha B)^r}{r!} \sum_{n=0}^{\infty} m_n = \exp(\alpha B) \sum_{n=0}^{\infty} m_n. \quad (24)$$

The cross section of the process then reads as

$$\sigma = \exp\left(2\alpha\left(B + \tilde{B}\right)\right) \hat{\sigma} = \exp(\delta_t) \hat{\sigma}, \quad (25)$$

where $\hat{\sigma}$ is the *hard process* cross section which is finite in the limit $\lambda \rightarrow 0$. The additional term in (25) \tilde{B} takes into account the infrared-divergent part of the real soft-photon emission:

$$\tilde{B} = -\frac{1}{8\pi^2} \int' \frac{d^3\mathbf{k}}{\sqrt{\mathbf{k}^2 + \lambda^2}} \left(\frac{p'_\mu}{(p'k)} - \frac{p_\mu}{(pk)} \right)^2, \quad (26)$$

where the accent at the integral denotes the region $|\mathbf{k}| < \omega$. The parameter ω is the maximum energy of real photons which escape undetected; it is defined by a specific experimental setup.

The sum of the contributions from the virtual and real soft-photon emission in (25) is

$$\delta_t \equiv 2\alpha(B + \tilde{B}) = -\frac{2\alpha}{\pi} (l_t - 1) \ln \frac{\sqrt{s}}{2\omega} + \frac{\alpha}{2\pi} l_t, \quad l_t = \ln \frac{-t}{m^2}, \quad (27)$$

This sum is infrared-stable, i.e. finite in the $\lambda \rightarrow 0$ limit, which is a manifestation of the well-known cancellation requirement of infrared singularities described by [24].

For Møller scattering (1), the soft-photon emission factor can be transformed in the following manner:

$$\begin{aligned} \left(-\frac{p_1^\mu}{(p_1k)} + \frac{p'_1{}^\mu}{(p'_1k)} - \frac{p_2^\mu}{(p_2k)} + \frac{p'_2{}^\mu}{(p'_2k)} \right)^2 &= \left(\frac{p_1^\mu}{(p_1k)} - \frac{p'_1{}^\mu}{(p'_1k)} \right)^2 + \left(\frac{p_2^\mu}{(p_2k)} - \frac{p'_2{}^\mu}{(p'_2k)} \right)^2 - \\ &- \left(\frac{p_1^\mu}{(p_1k)} - \frac{p_2^\mu}{(p_2k)} \right)^2 - \left(\frac{p'_1{}^\mu}{(p'_1k)} - \frac{p'_2{}^\mu}{(p'_2k)} \right)^2 + \\ &+ \left(\frac{p_1^\mu}{(p_1k)} - \frac{p'_2{}^\mu}{(p'_2k)} \right)^2 + \left(\frac{p_2^\mu}{(p_2k)} - \frac{p'_1{}^\mu}{(p'_1k)} \right)^2. \end{aligned} \quad (28)$$

Combining (25) and (27), we can now write out the infrared cancellation in the cross section in the form:

$$\sigma = \exp(2[\delta_t + \delta_u - \delta_s]) \hat{\sigma}, \quad (29)$$

where $\delta_{u,s}$ can be obtained from δ_t (see (27)) by replacing $l_t \rightarrow l_{u,s}$ with $l_u = \ln(-u/m^2)$ and $l_s = \ln(s/m^2)$. First term in the exponent (with δ_t) gives the contribution of the diagrams from Fig. 2(e) and 2(f), while δ_u represents diagrams from Fig. 2(c) and 2(d). Third term (with δ_s) corresponds to the diagrams from Fig. 2(a) and 2(b). Expanding this result on α/π , we get expressions identical to our previous formulas for the first order ((55) from [14])

$$\frac{\sigma^{\text{NLO}}}{\sigma^0} = \frac{2\alpha}{\pi} \ln \frac{4\omega^2}{s} \left(\ln \frac{tu}{m^2s} - 1 \right) + \dots \quad (30)$$

and the Q-part of the second order ((45) from [16])

$$\frac{\sigma_Q}{\sigma^0} = \frac{1}{2} \frac{\sigma^{\text{NNLO}} + \dots}{\sigma^0} = \frac{1}{2} \left(\frac{\alpha}{\pi} \right)^2 \left[2 \ln \frac{4\omega^2}{s} \left(\ln \frac{tu}{m^2s} - 1 \right) \right]^2 + \dots \quad (31)$$

To separate the "soft" and "hard" types of higher-order contributions, we use the factorized form of the cross section shown in (29). The "hard" contribution is essentially determined by the presence of the SM heavy bosons with large momentum q in loops; $m^2 \ll |q^2| \sim M_Z^2$, so we simplify calculations by neglecting the dependence on the external momenta.

V. CALCULATION OF HARD SUBDIAGRAMS

As it was shown in Section IV, the infrared-divergent terms are extracted from the amplitude as an exponential factor. We will refer to such contributions as *factorized*, and for them

$$\sigma_{ij}^f = \delta_f \sigma_{ij}^0, \quad ij = LL, RR, LR, 00. \quad (32)$$

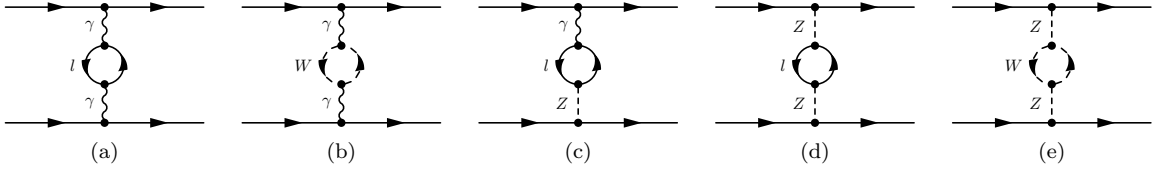


Figure 3: One-loop vacuum polarization diagrams.

If the physical contribution C to the observable asymmetry A is determined by the relative correction to the Born asymmetry,

$$\delta_A^C = (A^C - A^{(0)})/A^{(0)}, \quad (33)$$

then it is clear that these factorized contributions do not change the asymmetry, as they cancel each other in a ratio of a nominator to a denominator: $\delta_A^f = 0$. The contributions without the factorized property (32) will be referred to as *non-factorized*. The real physical cross section is the sum denoted by index $f + n$

$$\sigma_{ij}^{f+n} = \sigma_{ij}^f + \sigma_{ij}^n. \quad (34)$$

We should mention that in the general case $\delta_A^{f+n} \neq \delta_A^f + \delta_A^n = \delta_A^n$, but for the correct sum it is necessary to use the following formula:

$$\delta_A^{f+n} = \delta_A^n \frac{\sigma_{00}^0 + \sigma_{00}^n}{\sigma_{00}^0 + \sigma_{00}^f + \sigma_{00}^n} = \delta_A^n \left(1 - \frac{\delta_f}{1 + \delta_f + \delta_n} \right), \quad (35)$$

where $\delta_n = \sigma_{00}^n/\sigma_{00}^0$. It is the key formula we used for taking into consideration the radiative corrections up to the two-loop level. A recipe is very simple: the cross sections coming from the two-loop contributions are small, so 1) the relative corrections δ_f and δ_n from (35) are determined by the one-loop corrections, only 2) we add the two-loop contributions as *additive* terms (we used this terminology of our work [15]) of relative correction δ_A^n to the one-loop corrections obtained under firm control before (see, for example, our paper [14]). The contributions which should be evaluated explicitly are the hard subprocess terms (terms m_i from (22)). The contribution which comes from a photon emitted from an inner part of this hard diagram does not contain any infrared-divergent parts. As it is proven in [23], all infrared-divergent contributions come from diagrams with a virtual photon connecting outer legs of charged particles (see, for example, Fig. 4(a) – 4(f), Fig. 5(a) and Fig. 5(c)). Thus we only need to calculate the *Yennie–Frautschi–Suura–irreducible* (*YFS-irreducible*) diagrams as they do not contain contributions with a virtual photon connecting two external electron lines.

Another useful approximation we employ is including only hard virtual photons in $\hat{\sigma}$. This is similar to the factorization of soft and hard virtual corrections in the Drell–Yan cross section done in [25–27].

Except for the ultraviolet-divergent subdiagrams of vertex, lepton self-energy and boson vacuum polarization insertions, the skeleton contribution to m_i from (22) is ultraviolet-convergent. A regularization scheme must be applied to the ultraviolet-divergent subdiagrams; we use the on-shell renormalization scheme and the t’Hooft–Feynman gauge. Also, we assume that the loop momenta relevant to the skeleton amplitudes are large in comparison with the external momenta $|\chi^2| \gg s \sim -t \sim -u \gg m^2$, so we neglect the external momenta in m_i .

VI. ONE-LOOP RADIATIVE CORRECTIONS

The one-loop cross section was evaluated carefully and with full, firm control of the uncertainties in the literature; see, for example, our recent paper [14]. Here, we present some of the one-loop results which are relevant to this work; in particular, we want to compare the chiral amplitude method and the approach suggested in [14–16].

Vacuum polarizations of virtual photons which must be taken into account in m_i are shown by Fig. 3(a) and Fig. 3(b). For the bilinear combination of amplitudes entering the asymmetry in the Born approximation, this leads to the following replacement (see 20):

$$A_{\gamma SE} = A^{(0)}|_{A_0 \rightarrow \bar{A}_0}, \quad (36)$$

where

$$\bar{A}_0 = \frac{y(1-y)(A_t(1-y) + A_u y)}{(A_t(1-y) + A_u y)^2 + A_u^2 y^4 + A_t^2 (1-y)^4}. \quad (37)$$

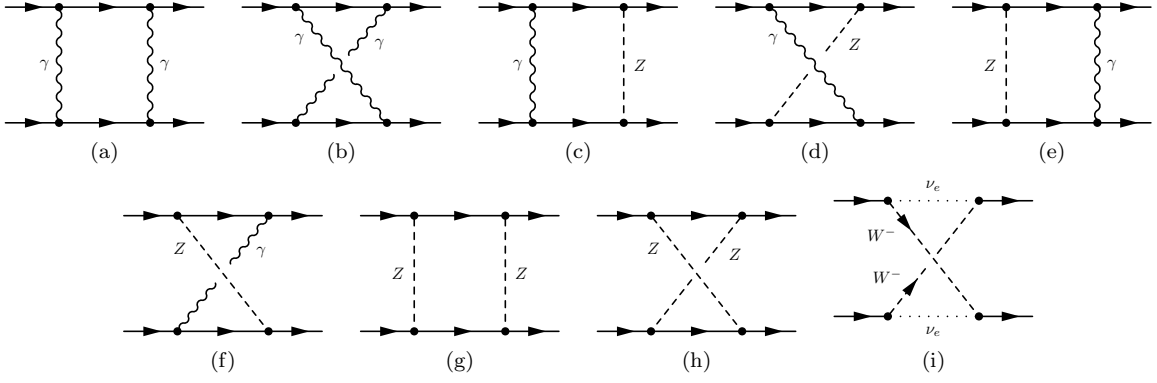


Figure 4: One-loop box type diagrams.

The self-energy (SE) factors associated with the t - and u -channels of the amplitudes in the Born approximation, A_t and A_u , have the form [19]:

$$A_t = \frac{1}{1 - \Pi_t}, \quad A_u = \frac{1}{1 - \Pi_u},$$

$$\Pi_t = \frac{\alpha}{3\pi} \left(l_t - \frac{5}{3} \right) + \frac{\alpha^2}{4\pi^2} \left(l_t + \zeta_3 - \frac{5}{24} \right) + \dots, \quad l_t = \ln \frac{-t}{m^2}.$$

$$\Pi_u = \Pi_t(l_t \rightarrow l_u),$$

where $\zeta_3 \approx 1.202$ is the Riemann zeta function. The asymmetry that includes the Born approximation as well as the first- and the second-order corrections can be written as: $A = A_{\gamma SE} \left(1 + \frac{\alpha}{\pi} \delta_1 + \left(\frac{\alpha}{\pi} \right)^2 \delta_2 \right)$. The term δ_1 contains contributions from the one-loop diagrams with two- Z , WZ , and WW exchange, as well as the vertex functions of leptons with the Z and W bosons in the intermediate state. The term δ_2 contains contributions from the self-energy insertions into the lepton functions with W and Z boson exchanges, boson vacuum polarizations and two-loop Feynman diagrams of two types – double-box and decorated-box.

The contribution to the vacuum polarization from the W -boson in the intermediate state A_γ^Π (Fig. 3 (b) and (e)) does not add anything to the asymmetry as it has the same form for the $(---)$ and $(+++)$ spiral states:

$$A_\gamma^\Pi = 0.$$

With our approach, we only need to consider the YFS-irreducible diagrams, i.e. we can omit the contributions from the YFS-reducible diagrams Fig. 4(a) – 4(f). Thus it is sufficient to consider only one diagram with crossed W -legs, shown in Fig. 4(i), which contributes to the \mathcal{M}^{----} amplitude. The other two, Fig. 4(g) and Fig. 4(h), lead to the second term in \mathcal{M}_Z^0 from (16). Let us start with the WW crossed box:

$$2\mathcal{M}_B^* \mathcal{M}_{WW} = 4s^4 (-4\alpha\pi i) \frac{(4\pi\alpha)^2 i\pi^2}{4s_W^4 (2\pi)^4} (\mathcal{M}_\gamma^0)^* \mathcal{M}_Z^0 N_{WW} \frac{1}{M_Z^2}, \quad (38)$$

where $s_W = \sin \theta_W$, $c_W = \cos \theta_W$ and

$$N_{WW} = \frac{M_W^2}{s^2 t} \int d\chi \frac{S_{WW}}{(\chi^2)^2 (\chi^2 - M_W^2)^2}, \quad d\chi = \frac{d^4 \chi}{i\pi^2}, \quad (39)$$

$$S_{WW} = \text{Sp} [\hat{p}'_1 \gamma_\mu \hat{\chi} \gamma_\nu \hat{p}_1 \hat{p}'_2 \hat{p}'_2 \gamma^\nu \hat{\chi} \gamma^\mu \hat{p}_2 \hat{p}_1 \omega_-] = 2\chi^2 s^2 t.$$

We use a Wick rotation to perform the loop momenta integration in (39):

$$d\chi \rightarrow \chi_e^2 d\chi_e^2, \quad \text{where} \quad \chi^2 = -\chi_e^2 < 0. \quad (40)$$

Evaluating the integral, we obtain $N_{WW} = -2$. Thus, the resultant contribution to the asymmetry is:

$$A_{WW} = \frac{\alpha}{\pi} \bar{A}_0 \frac{s}{8M_W^2 s_W^4}. \quad (41)$$

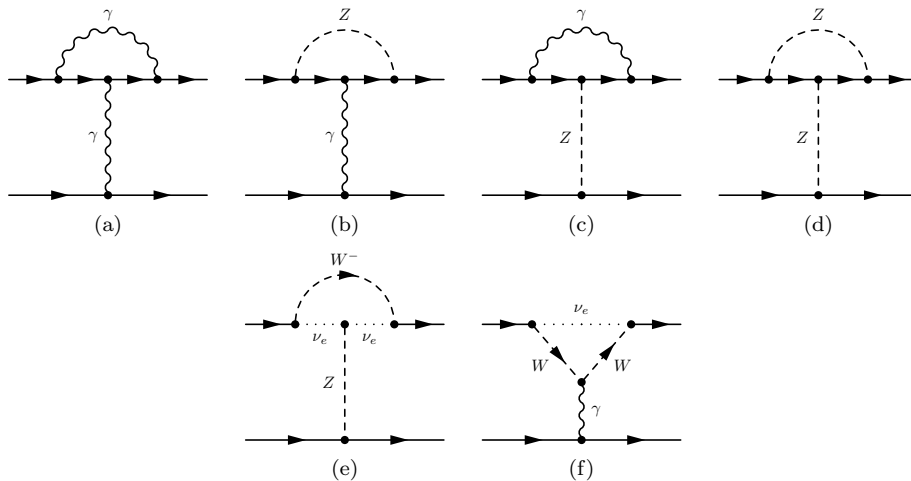


Figure 5: One-loop vertex correction diagrams.

This result is in full agreement with the relative correction to the asymmetry induced by a WW -box obtained in [15] (see formula (40) there): $A_{WW} = \delta_A^{WW} A^{(0)}$, where δ_A^C is determined by (33). For all *non-factorized* two-loop corrections, the formula connecting the relative correction δ_A^C with the asymmetry induced by the effect C is

$$A_C = \delta_A^C A^{(0)}. \quad (42)$$

A contribution from the ZZ box and crossed ZZ box diagrams, (Fig. 4(g) and 4(h)), has a similar form:

$$A_{ZZ} = -\frac{\alpha}{\pi} \bar{A}_0 \frac{s}{M_Z^2} \frac{a_V}{32c_W^4 s_W^4} N_{ZZ}, \quad N_{ZZ} = 6. \quad (43)$$

Similarly to the WW -box case, the relative correction to the asymmetry induced by a ZZ -box obtained in [15] is in perfect agreement with the result presented here: $A_{ZZ} = \delta_A^{ZZ} A^{(0)}$.

It also is necessary to take into account the contribution of the vertex function of the electron coming from the W - and Z -boson exchange (see Fig. 5). The diagrams of Fig. 5(a) and Fig. 5(c) are YFS-reducible and should be omitted to avoid double-counting. It is important to note that in comparison to the contribution from Fig. 5(b) and 5(f), the contributions from Fig. 5(d) and 5(e) contain an additional factor of (t/M_Z^2) . Using explicit expressions for the corresponding contributions to the vertex functions given in Appendix B, we obtain the following contributions to the asymmetry:

$$A_Z^\Gamma = \frac{\alpha}{\pi} \bar{A}_0 \frac{s}{12M_Z^2} \frac{a_V}{c_W^2 s_W^2} \left(\ln \frac{M_Z^4}{tu} + \frac{17}{3} \right), \quad (44)$$

$$A_W^\Gamma = -\frac{\alpha}{\pi} \bar{A}_0 \frac{s}{M_Z^2} \frac{1}{c_W^2 s_W^2} \frac{34}{9}. \quad (45)$$

Again, the asymptotic relative correction to the Z -boson vertex function obtained in [15] agrees with the result presented here: $A_Z^\Gamma \approx \delta_A^{\Lambda_2} A^{(0)}$.

VII. TWO-LOOP BOX RADIATIVE CORRECTIONS

It is convenient to divide the two-loop box contributions discussed here into three types: one type including boxes with lepton self-energy diagrams, and two other types corresponding to the ladder and decorated-box type.

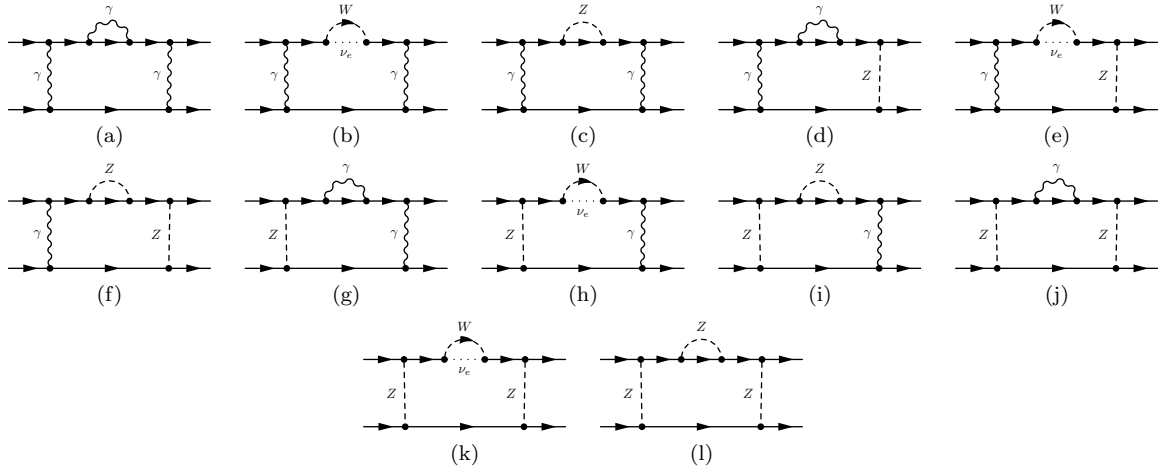


Figure 6: One-loop direct box type diagrams with lepton self energy corrections.

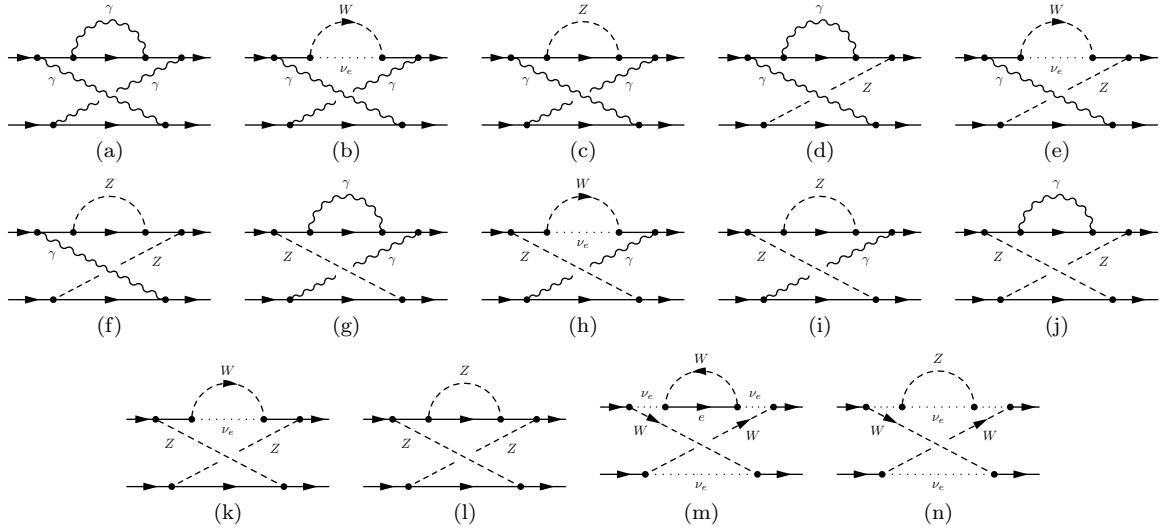


Figure 7: One-loop crossed box type diagrams with lepton self energy corrections.

A. Boxes with lepton self-energy

For fermions with polarization $\lambda = \pm$, the mass operator has the form [28]:

$$\begin{aligned}
 \mathcal{M}_-(p)\omega_- &= -\frac{p^2\hat{p}}{8\pi^2}\omega_- \left[\left(\frac{g(1-a_V)}{4c_W} \right)^2 J_Z + \frac{g^2}{2} J_W \right], \\
 \mathcal{M}_+(p)\omega_+ &= -\frac{p^2\hat{p}}{8\pi^2}\omega_+ \left(\frac{g(1+a_V)}{4c_W} \right)^2 J_Z, \\
 \mathcal{M}_-(p)\omega_- &= -\frac{p^2\hat{p}}{8\pi^2}\omega_- \frac{g^2}{2} J_W,
 \end{aligned} \tag{46}$$

where, based on the approach developed in [28] for the pure QED case,

$$\begin{aligned}
 J_Z &= J_Z(p^2) = \int_0^1 dx \int_0^1 dz \frac{x(1-x)}{M_Z^2 - p^2xz}, \\
 J_W &= J_Z(M_Z \rightarrow M_W).
 \end{aligned} \tag{47}$$

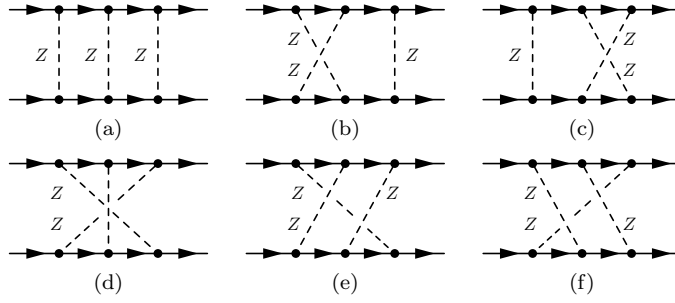


Figure 8: Double-box-type diagrams with ZZZ exchange (see Section VIII B 1).

Let us evaluate the contribution to the asymmetry coming from self-energy insertions into the lepton lines (e, ν) in the two-boson $\gamma\gamma, \gamma Z, ZZ, WW$ exchange amplitudes (all of them are presented in Figs. 6 and 7)

:

$$A_{\Sigma} = A_{\gamma Z}^Z + A_{\gamma Z}^W + A_{WW}^{\nu}. \quad (48)$$

For $A_{\gamma Z}^Z$, we have

$$A_{\gamma Z}^Z = -\left(\frac{\alpha}{\pi}\right)^2 \bar{A}_0 \frac{24s_{\alpha V}}{M_Z^2} \rho^2 \mathcal{J}_Z, \quad L_Z = \ln \frac{M_Z^2}{m^2}, \quad \rho = \frac{1}{4c_W s_W}, \quad (49)$$

$$\mathcal{J}_Z = \frac{1}{6} L_Z + \int_0^1 dx x \bar{x} \int_0^1 dz \left\{ -\ln \beta + \rho^2 \int_0^{\infty} \frac{dt}{1+\beta t} \left[\frac{4}{t+1} + \frac{3\rho^2 t}{(t+1)^2} \right] \right\} = \frac{1}{6} L_Z + 0.888, \quad (50)$$

where $\bar{x} = 1 - x$ and $\beta = xz$. The intermediate W state in the electron self-energy gives

$$A_{\gamma Z}^W = \left(\frac{\alpha}{\pi}\right)^2 \bar{A}_0 \frac{3s}{M_Z^2 s_W^2} \mathcal{J}_W, \quad L_W = \ln \frac{M_W^2}{m^2}, \quad a = \frac{1}{c_W^2}, \quad (51)$$

$$\mathcal{J}_W = \frac{1}{6} L_W + \int_0^1 dx x \bar{x} \int_0^1 dz \left\{ -\ln \beta + \rho^2 \int_0^{\infty} \frac{dt}{1+\beta t} \left[\frac{2}{t+a} + \frac{\rho^2}{(t+a)^2} \right] \right\} = \frac{1}{6} L_W + 0.542. \quad (52)$$

The contribution from the neutrino self-energy insertion is

$$A_{WW}^{\nu} = \left(\frac{\alpha}{\pi}\right)^2 \bar{A}_0 \frac{s}{8M_Z^2 s_W^6 c_W^2} R^{\nu}, \quad (53)$$

where

$$R^{\nu} = \int_0^1 dx x \bar{x} \int_0^1 dz \int_0^{\infty} \frac{tdt}{(t+1)^2} \left(\frac{1}{a+\beta t} + \frac{2c_W^2}{1+\beta t} \right) = 0.586. \quad (54)$$

B. Ladder-box diagrams

1. ZZZ exchange

The contribution of the ladder-box diagrams with an exchange of three Z bosons (Figs. 8(a)-8(f)) to the asymmetry has the form:

$$A_{ZZZ} = \left(\frac{\alpha}{\pi}\right)^2 \bar{A}_0 \frac{3s_{\alpha V}}{M_Z^2} \rho^6 N_{ZZZ}, \quad (55)$$

where N_{ZZZ} is the loop momentum integral:

$$N_{ZZZ} = N_{123}^{ZZZ} + N_{132}^{ZZZ} + N_{213}^{ZZZ} + N_{321}^{ZZZ} + N_{312}^{ZZZ} + N_{231}^{ZZZ} = 2.40755, \quad (56)$$

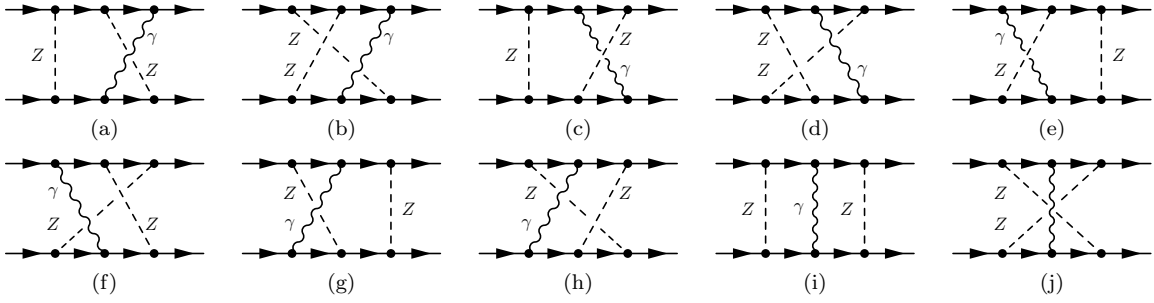


Figure 9: Double-box-type diagrams with $ZZ\gamma$ exchange (see Section VIIB 2).

which includes 6 terms corresponding to 6 diagrams with three Z -boson exchanges:

$$\text{Fig. 8(a) : } N_{123}^{ZZZ} = \int \frac{d\chi M_Z^2}{\mathbf{a}_e^2 \mathbf{b}_e^2 \mathbf{a}_Z \mathbf{b}_Z \mathbf{c}_Z} S_{123} = -59.8697, \quad (57)$$

$$\text{Fig. 8(b) : } N_{132}^{ZZZ} = \int \frac{d\chi M_Z^2}{\mathbf{a}_e \mathbf{b}_e^2 \mathbf{c}_e \mathbf{a}_Z \mathbf{b}_Z \mathbf{c}_Z} S_{132} = 16.6497, \quad (58)$$

$$\text{Fig. 8(c) : } N_{213}^{ZZZ} = \int \frac{d\chi M_Z^2}{\mathbf{a}_e^2 \mathbf{b}_e \mathbf{c}_e \mathbf{a}_Z \mathbf{b}_Z \mathbf{c}_Z} S_{213} = 16.6497, \quad (59)$$

$$\text{Fig. 8(d) : } N_{321}^{ZZZ} = \int \frac{d\chi M_Z^2}{\mathbf{a}_e^2 \mathbf{b}_e^2 \mathbf{a}_Z \mathbf{b}_Z \mathbf{c}_Z} S_{321} = -4.32159, \quad (60)$$

$$\text{Fig. 8(e) : } N_{312}^{ZZZ} = \int \frac{d\chi M_Z^2}{\mathbf{a}_e^2 \mathbf{b}_e \mathbf{c}_e \mathbf{a}_Z \mathbf{b}_Z \mathbf{c}_Z} S_{312} = 16.6497, \quad (61)$$

$$\text{Fig. 8(f) : } N_{231}^{ZZZ} = \int \frac{d\chi M_Z^2}{\mathbf{a}_e \mathbf{b}_e^2 \mathbf{c}_e \mathbf{a}_Z \mathbf{b}_Z \mathbf{c}_Z} S_{231} = 16.6497. \quad (62)$$

Here we use traces and notations defined in Appendix D. The loop momentum integrals and notations for the propagator denominators are defined in Appendix E.

2. $ZZ\gamma$ and $WW\gamma$ exchange

The contribution of the double-box diagrams with one photon and two Z -boson exchanges (Fig. 9) to the asymmetry has the form:

$$A_{ZZ\gamma} = -\left(\frac{\alpha}{\pi}\right)^2 \bar{A}_0 \frac{2sa_V}{M_Z^2} \rho^4 N_{ZZ\gamma}, \quad (63)$$

where $N_{ZZ\gamma}$ is the loop momentum integral

$$\begin{aligned} N_{ZZ\gamma} &= N_{213}^{ZZ\gamma} + N_{312}^{ZZ\gamma} + N_{213}^{ZZ\gamma} + N_{231}^{ZZ\gamma} + N_{132}^{ZZ\gamma} + N_{231}^{ZZ\gamma} + N_{132}^{ZZ\gamma} + N_{312}^{ZZ\gamma} + N_{123}^{ZZ\gamma} + N_{321}^{ZZ\gamma} = \\ &= 8L_Z + 61.2176, \end{aligned} \quad (64)$$

which includes 10 terms corresponding to 10 diagrams with one photon and two Z -boson exchanges:

$$\text{Fig. 9(a) : } N_{213}^{ZZ\gamma} = \int \frac{d\chi M_Z^2}{\mathbf{a}_e^2 \mathbf{b}_e \mathbf{c}_e \mathbf{a}_Z \mathbf{b}_Z \mathbf{c}_Z} S_{213} = 13.1595, \quad (65)$$

$$\text{Fig. 9(b) : } N_{312}^{ZZ\gamma} = \int \frac{d\chi M_Z^2}{\mathbf{a}_e^2 \mathbf{b}_e \mathbf{c}_e \mathbf{a}_Z \mathbf{b}_Z \mathbf{c}_Z} S_{312} = 13.1595, \quad (66)$$

$$\text{Fig. 9(c) : } N_{213}^{ZZ\gamma} = \int \frac{d\chi M_Z^2}{\mathbf{a}_e^2 \mathbf{b}_e \mathbf{c}_e \mathbf{a}_Z \mathbf{b}_Z \mathbf{c}_Z} S_{213} = 39.4784, \quad (67)$$

$$\text{Fig. 9(d) : } N_{231}^{ZZ\gamma} = \int \frac{d\chi M_Z^2}{\mathbf{a}_e \mathbf{b}_e^2 \mathbf{c}_e \mathbf{a}_Z \mathbf{b}_Z \mathbf{c}_Z} S_{231} = 4L_Z + 19.7392, \quad (68)$$

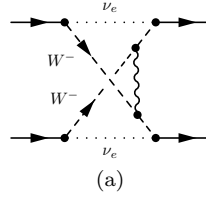


Figure 10: Double-box-type diagrams of ladder form $WW\gamma$ exchange (see Section VII B 2).

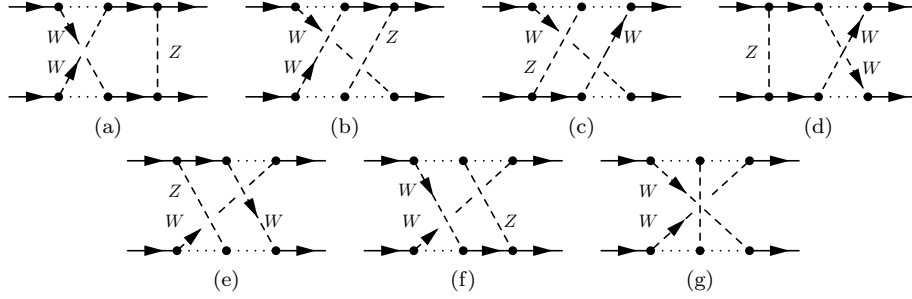


Figure 11: Double-box-type diagrams with ZWW exchange (see Section VII B 3).

$$\text{Fig. 9(e)} : \quad N_{132}^{ZZ\gamma} = \int \frac{d\chi M_Z^2}{\mathbf{a}_e \mathbf{b}_e^2 \mathbf{c}_e \mathbf{a} \mathbf{b}_Z \mathbf{c}_Z} S_{132} = 13.1595, \quad (69)$$

$$\text{Fig. 9(f)} : \quad N_{231}^{ZZ\gamma} = \int \frac{d\chi M_Z^2}{\mathbf{a}_e \mathbf{b}_e^2 \mathbf{c}_e \mathbf{a} \mathbf{b}_Z \mathbf{c}_Z} S_{231} = 13.1595, \quad (70)$$

$$\text{Fig. 9(g)} : \quad N_{132}^{ZZ\gamma} = \int \frac{d\chi M_Z^2}{\mathbf{a}_e \mathbf{b}_e^2 \mathbf{c}_e \mathbf{a}_Z \mathbf{b}_Z \mathbf{c}} S_{132} = 4L_Z + 19.7392, \quad (71)$$

$$\text{Fig. 9(h)} : \quad N_{312}^{ZZ\gamma} = \int \frac{d\chi M_Z^2}{\mathbf{a}_e^2 \mathbf{b}_e \mathbf{c}_e \mathbf{a}_Z \mathbf{b}_Z \mathbf{c}} S_{312} = 39.4784, \quad (72)$$

$$\text{Fig. 9(i)} : \quad N_{123}^{ZZ\gamma} = \int \frac{d\chi M_Z^2}{\mathbf{a}_e^2 \mathbf{b}_e^2 \mathbf{a}_Z \mathbf{b}_Z \mathbf{c}} S_{123} = -105.276, \quad (73)$$

$$\text{Fig. 9(j)} : \quad N_{321}^{ZZ\gamma} = \int \frac{d\chi M_Z^2}{\mathbf{a}_e^2 \mathbf{b}_e^2 \mathbf{a}_Z \mathbf{b}_Z \mathbf{c}} S_{321} = -4.57974. \quad (74)$$

As before, we use traces and notations defined in Appendix D and the loop momentum integrals and notations for the propagator denominators defined in Appendix E.

The contribution of the double-box diagrams of ladder form with one-photon exchange between two W -bosons (Fig. 10) is given by:

$$A_{WW\gamma} = - \left(\frac{\alpha}{\pi} \right)^2 \bar{A}_0 \frac{s}{16M_Z^2} \frac{1}{s_W^4 c_W^2} N_{WW\gamma}, \quad (75)$$

where $N_{WW\gamma}$ is the loop momentum integral

$$N_{WW\gamma} = \int \frac{d\chi M_W^2}{\mathbf{a}_e \mathbf{c}_e \mathbf{a}_W^2 \mathbf{c}_W^2 \mathbf{b}} S_{WW\gamma} = 11.1595, \quad (76)$$

and the trace $S_{WW\gamma}$ is presented in (D17).

3. ZWW exchange

The contribution of the double-box diagrams with one photon and two Z -bosons exchanges, presented in Fig. 11, can be expressed as:

$$A_{ZWW} = - \left(\frac{\alpha}{\pi} \right)^2 \bar{A}_0 \frac{s}{16M_Z^2} \frac{\rho^2}{s_W^4} N_{ZWW}, \quad (77)$$

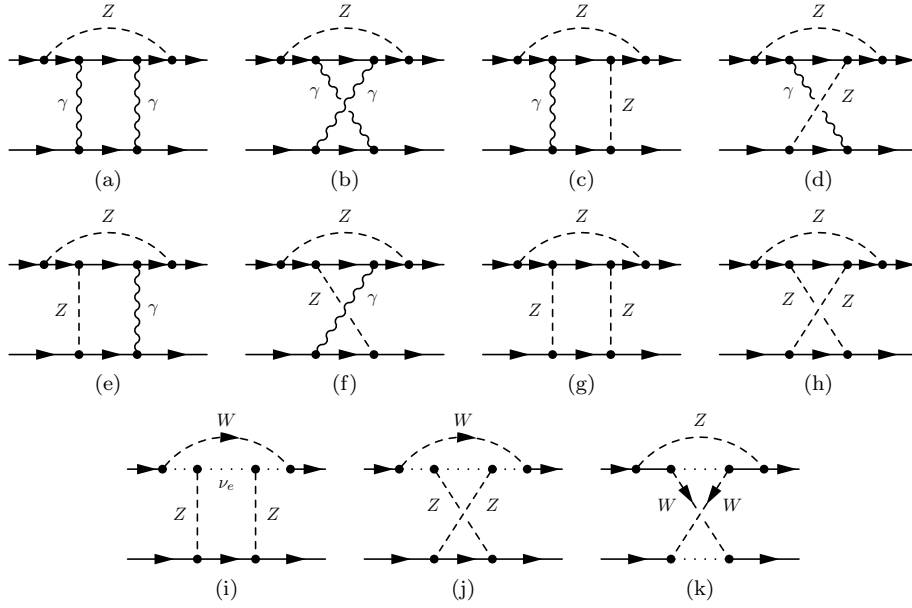


Figure 12: Decorated box diagrams of Type I (see Section VII C 1).

where N_{ZWW} is the loop momentum integral,

$$N_{ZWW} = N_{132}^{ZWW} + N_{312}^{ZWW(1)} + N_{312}^{ZWW(2)} + N_{213}^{ZWW} + N_{231}^{ZWW(1)} + N_{231}^{ZWW(2)} + N_{321}^{ZWW} = -24.4674, \quad (78)$$

which includes 7 terms corresponding to 7 diagrams with one Z -boson and two W -boson exchanges:

$$\text{Fig. 11(a)} : \quad N_{132}^{ZWW} = \int \frac{d\chi M_Z^2}{\mathbf{b}_e^2 \mathbf{a}_W \mathbf{b}_Z \mathbf{c}_W \mathbf{a} \mathbf{c}} S_{132} = 8.52405, \quad (79)$$

$$\text{Fig. 11(b)} : \quad N_{312}^{ZWW(1)} = \int \frac{d\chi M_Z^2}{\mathbf{b}_e \mathbf{a}_W \mathbf{b}_Z \mathbf{c}_W \mathbf{a}^2 \mathbf{c}} S_{312} = -27.2451, \quad (80)$$

$$\text{Fig. 11(c)} : \quad N_{312}^{ZWW(2)} = \int \frac{d\chi M_Z^2}{\mathbf{c}_e \mathbf{a}_W \mathbf{b}_W \mathbf{c}_Z \mathbf{a}^2 \mathbf{b}} S_{312} = 9.08169, \quad (81)$$

$$\text{Fig. 11(d)} : \quad N_{213}^{ZWW} = \int \frac{d\chi M_Z^2}{\mathbf{a}_e^2 \mathbf{a}_Z \mathbf{b}_W \mathbf{c}_W \mathbf{b} \mathbf{c}} S_{213} = 8.52405, \quad (82)$$

$$\text{Fig. 11(e)} : \quad N_{231}^{ZWW(1)} = \int \frac{d\chi M_Z^2}{\mathbf{a}_e \mathbf{a}_Z \mathbf{b}_W \mathbf{c}_W \mathbf{b}^2 \mathbf{c}} S_{231} = -27.2451, \quad (83)$$

$$\text{Fig. 11(f)} : \quad N_{231}^{ZWW(2)} = \int \frac{d\chi M_Z^2}{\mathbf{c}_e \mathbf{a}_W \mathbf{b}_W \mathbf{c}_Z \mathbf{a} \mathbf{b}^2} S_{231} = 9.08169, \quad (84)$$

$$\text{Fig. 11(g)} : \quad N_{321}^{ZWW} = \int \frac{d\chi M_Z^2}{\mathbf{a}_W \mathbf{b}_W \mathbf{c}_Z \mathbf{a}^2 \mathbf{b}^2} S_{321} = -5.18876, \quad (85)$$

where the traces S_{132}, \dots coincide with the traces from the ZZZ case (see Appendix D).

C. Decorated-box diagrams

1. Type I

The contribution to the asymmetry coming from the decorated-box diagrams with two photon exchanges, presented in Fig. 12(a) and 12(b), has the form:

$$A_{\gamma\gamma}^Z = \left(\frac{\alpha}{\pi}\right)^2 \bar{A}_0 \frac{2sa_V}{M_Z^2} \rho^2 N_{\gamma\gamma}^Z, \quad (86)$$

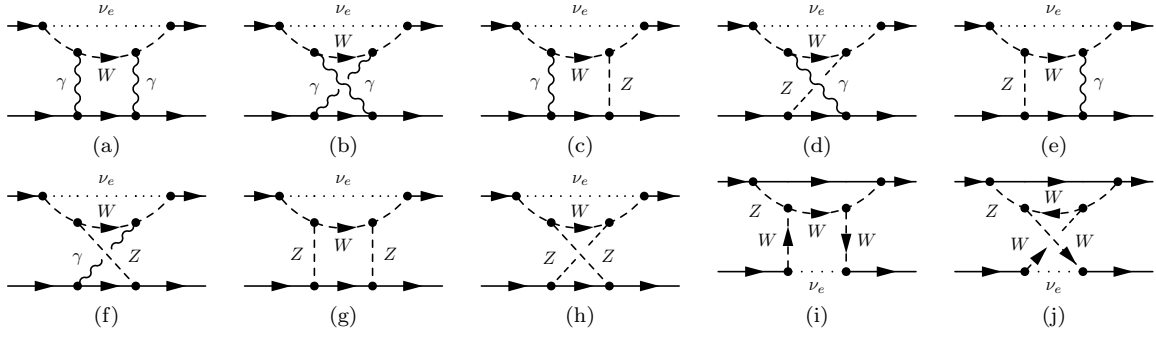


Figure 13: Decorated box diagrams of Type II (see Section VII C 2).

where $N_{\gamma\gamma}^Z$ is the loop momentum integral:

$$N_{\gamma\gamma}^Z = \int \frac{d\chi M_Z^2}{\mathbf{a}_e^2 \mathbf{b}_e^2 \mathbf{c}_e \mathbf{a}_Z \mathbf{b}^2} (S_1^I + S_2^I) = [2L_Z^2 + 6L_Z + 13.1595] + [-2L_Z^2 - 13.6595] = 6L_Z - 0.5, \quad (87)$$

and the traces $S_{1,2}^I$ are defined in Appendix D. The contribution of decorated-box diagrams with one photon and one Z-boson exchange (Fig. 12(c), 12(d), 12(e) and 12(f)) is given by:

$$A_{\gamma Z}^Z = -\left(\frac{\alpha}{\pi}\right)^2 \bar{A}_0 \frac{16sa_V}{M_Z^2} \rho^4 N_{\gamma Z}^Z, \quad N_{\gamma Z}^Z = \int \frac{d\chi M_Z^2}{\mathbf{a}_e^2 \mathbf{b}_e^2 \mathbf{c}_e \mathbf{a}_Z \mathbf{b}_Z \mathbf{b}} (S_1^I + S_2^I) = 8.57974. \quad (88)$$

The decorated-box diagrams with two Z-boson exchanges (Fig. 12(g) and 12(h)) contribute the following:

$$A_{ZZ}^Z = -\left(\frac{\alpha}{\pi}\right)^2 \bar{A}_0 \frac{6sa_V}{M_Z^2} \rho^6 N_{ZZ}^Z, \quad N_{ZZ}^Z = \int \frac{d\chi M_Z^2}{\mathbf{a}_e^2 \mathbf{b}_e^2 \mathbf{c}_e \mathbf{a}_Z \mathbf{b}_Z^2} (S_1^I + S_2^I) = 5.15947. \quad (89)$$

The decorated-box diagrams with two Z-boson exchanges (Fig. 12(i) and 12(j)) give the term:

$$A_{ZZ}^W = -\left(\frac{\alpha}{\pi}\right)^2 \bar{A}_0 \frac{s}{M_Z^2} \frac{\rho^4}{s_W^2} N_{ZZ}^W, \quad N_{ZZ}^W = \int \frac{d\chi M_Z^2}{\mathbf{a}^2 \mathbf{b}_e \mathbf{c} \mathbf{a}_W \mathbf{b}_Z^2} (S_1^I + S_2^I) = 5.86885. \quad (90)$$

And, finally, the contribution to the asymmetry from the decorated-box diagrams with two W-boson exchanges, presented in Fig. 12(k), has the form:

$$A_{WW}^Z = -\left(\frac{\alpha}{\pi}\right)^2 \bar{A}_0 \frac{s}{M_Z^2} \frac{\rho^2}{8s_W^4} N_{WW}^Z, \quad N_{WW}^Z = \int \frac{d\chi M_Z^2}{\mathbf{a}_e^2 \mathbf{b} \mathbf{c} \mathbf{a}_Z \mathbf{b}_W^2} S_2^I = -11.7914. \quad (91)$$

2. Type II

The contribution to the asymmetry from the decorated-box diagrams with two photon exchanges, presented in Fig. 13(a) and 13(b), has the form:

$$A_{\gamma\gamma}^W = -\left(\frac{\alpha}{\pi}\right)^2 \bar{A}_0 \frac{s}{4M_Z^2} \frac{1}{s_W^2} N_{\gamma\gamma}^W, \quad N_{\gamma\gamma}^W = \int \frac{d\chi M_Z^2}{\mathbf{a} \mathbf{b}^2 \mathbf{a}_W^2 \mathbf{c}_W \mathbf{b}_e} (S_1^{II} + S_2^{II}) = \frac{1}{c_W^2} \left(\frac{29}{2} L_W + 27.9711 \right), \quad (92)$$

with the trace $S_{1,2}^{II}$ defined in Appendix D. The decorated-box diagrams with one photon and one Z-boson exchange, presented in Fig. 13(c), 13(d), 13(e) and 13(f), contribute the following:

$$A_{\gamma Z}^W = -\left(\frac{\alpha}{\pi}\right)^2 \bar{A}_0 \frac{s}{2M_Z^2} \frac{\rho c_W}{s_W^3} N_{\gamma Z}^W, \quad N_{\gamma Z}^W = \int \frac{d\chi M_Z^2}{\mathbf{a} \mathbf{b} \mathbf{b}_e \mathbf{a}_W^2 \mathbf{b}_Z \mathbf{c}_W} (S_1^{II} + S_2^{II}) = 43.8282. \quad (93)$$

The decorated-box diagrams with two Z-boson exchanges (Fig. 13(g) and 13(h)) add the term:

$$A_{ZZ}^W = -\left(\frac{\alpha}{\pi}\right)^2 \bar{A}_0 \frac{s}{4M_Z^2} \frac{\rho^2}{s_W^4} N_{ZZ}^W, \quad N_{ZZ}^W = \int \frac{d\chi M_Z^2}{\mathbf{a} \mathbf{b}_e \mathbf{a}_W^2 \mathbf{b}_Z^2 \mathbf{c}_W} (S_1^{II} + S_2^{II}) = 22.4637. \quad (94)$$

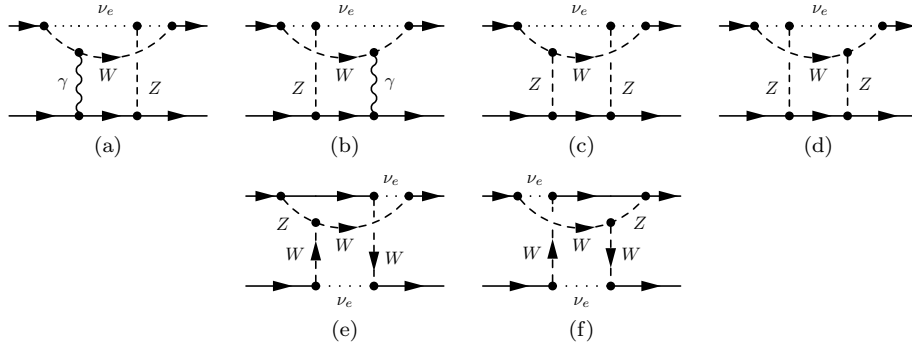


Figure 14: Decorated box diagrams of Type III (see Section VII C 3).

The contribution to the asymmetry from the decorated-box diagrams with two W -boson exchanges (Fig. 13(i) and 13(j)) is given by:

$$A_{WW}^W = -\left(\frac{\alpha}{\pi}\right)^2 \bar{A}_0 \frac{s}{4M_Z^2} \rho^2 \frac{c_W^2}{s_W^4} N_{WW}^W, \quad N_{WW}^W = \int \frac{d\chi M_Z^2}{\mathbf{a}_e \mathbf{b} \mathbf{a}_Z^2 \mathbf{b}_W^2 \mathbf{c}_W} (S_1^{II} + S_2^{II}) = 28.9044. \quad (95)$$

3. Type III

The decorated-box diagrams with one photon and one Z -boson exchange, presented in Fig. 14(a) and 14(b), give the following contribution to the asymmetry:

$$A_{\gamma Z}^W = \left(\frac{\alpha}{\pi}\right)^2 \bar{A}_0 \frac{s}{2M_Z^2} \frac{\rho^2}{s_W^2} N_{\gamma Z}^W, \quad N_{\gamma Z}^W = \int \frac{d\chi M_Z^2}{\mathbf{a} \mathbf{b} \mathbf{c} \mathbf{c}_e \mathbf{a}_W \mathbf{b}_W \mathbf{c}_Z} (S_1^{III} + S_2^{III}) = -6.67531, \quad (96)$$

with the trace $S_{1,2}^{III}$ defined in Appendix D. The decorated-box diagrams with two Z -boson exchanges (Fig. 14(c) and 14(d)) add the following:

$$A_{ZZ}^W = \left(\frac{\alpha}{\pi}\right)^2 \bar{A}_0 \frac{s}{2M_Z^2} \frac{\rho^3}{s_W^3} N_{ZZ}^W, \quad N_{ZZ}^W = \int \frac{d\chi M_Z^2}{\mathbf{a} \mathbf{b} \mathbf{c}_e \mathbf{a}_W \mathbf{b}_W \mathbf{c}_Z^2} (S_1^{III} + S_2^{III}) = 122.355. \quad (97)$$

Finally, the contribution to the asymmetry from the decorated-box diagrams with two W -boson exchanges (Fig. 14(e) and 14(f)) has the form:

$$A_{WW}^Z = \left(\frac{\alpha}{\pi}\right)^2 \bar{A}_0 \frac{s}{8M_Z^2} \frac{\rho c_W}{s_W^5} N_{WW}^Z, \quad (98)$$

$$N_{WW}^Z = \int d\chi M_Z^2 \left(\frac{S_1^{III}}{\mathbf{a} \mathbf{b}_e \mathbf{c} \mathbf{a}_W \mathbf{b}_Z \mathbf{c}_W^2} + \frac{S_2^{III}}{\mathbf{a}_e \mathbf{b} \mathbf{c} \mathbf{a}_Z \mathbf{b}_W \mathbf{c}_W^2} \right) = -3.25915. \quad (99)$$

VIII. NUMERICAL ESTIMATION OF TWO-LOOP EFFECTS TO ASYMMETRY

Gathering the contributions from the different Feynman diagrams considered in this paper, we notice the following structure of the PV asymmetry A :

$$A = -\bar{A}_0 \frac{s}{M_Z^2} \left\{ a_V \left[R_B^Z + \frac{\alpha}{\pi} R_{(1)}^Z + \left(\frac{\alpha}{\pi}\right)^2 R_{(2)}^Z + \dots \right] + \frac{\alpha}{\pi} R_{(1)}^W + \left(\frac{\alpha}{\pi}\right)^2 R_{(2)}^W + \dots \right\}, \quad (100)$$

where R_B^Z is the Born-level contribution to the asymmetry (20) and $R_{(1,2)}^{Z,W}$ come from the one- and two-loop radiative corrections respectively:

$$\begin{aligned} R_B^Z &= \frac{1}{2c_W^2 s_W^2} \approx \frac{8}{3} = 2.66, \\ R_{(1)}^Z &= 0.93775 \ln \frac{M_Z^4}{tu} - 0.622, \quad R_{(1)}^W = -33.4253, \\ R_{(2)}^Z &= -0.834656 L_Z + 40.9947, \quad R_{(2)}^W = 20.3961 L_W - 2.16291 L_Z + 99.5243. \end{aligned} \quad (101)$$

Translating this result to the language of the relative corrections, we can say that the general effect of all the box contributions gives $\delta_A = -0.93\%$. The main contribution to this value comes from the decorated box in Fig. 13 (a) and (b), -0.91% . The other contributions do not exceed $\sim 0.22\%$ and partially cancel each other. Now, combining this value with the well-known one-loop electroweak corrections [14] according to the formula (35), we obtain $\delta_A = (-0.93\%) \times 1.4514 = -1.35\%$ for the central point of MOLLER kinematics. Since the combined statistical and systematic uncertainty of MOLLER is $\delta_A^{\text{exp}} \sim \pm 2\%$, one can clearly see that it is essential to include the two-loop radiative corrections.

IX. CONCLUSION

Experimental investigation of Møller scattering is not only one of the oldest tools of modern physics in the framework of the Standard Model, but also a powerful probe of new physics effects. The new ultra-precise measurement of the weak mixing angle via 11 GeV Møller scattering planned soon at JLab, named MOLLER, as well as experiments planned at the ILC, will require the higher-order effects to be taken into account with the highest precision.

In this work, using the on-shell renormalization scheme and the t'Hooft–Feynman gauge, we evaluate the electroweak radiative corrections to the parity-violating asymmetry in the Møller scattering cross section and account for some NNLO contributions arising from the two-loop topology of Feynman diagrams. As one can see from our numerical data, at the MOLLER kinematic conditions the part of the NNLO EWC we considered in this work can decrease the asymmetry by up to $\sim 1\%$.

Since the focus of this work is the two-loop box diagrams, we do not consider the contributions arising from the SM corrections to the $W e \nu_e$ and $W e e$ vertices, as well as SM contributions to the boson self-energies; however, they will need to be addressed in the future. We plan to continue work in this direction and hope to provide a more precise result at some later time.

Appendix A: Feynman Rules in Standard Model

Below we summarize a set of the SM Feynman rules relevant to our calculation of the box diagrams. The lepton and the vector-boson propagators are:

$$\frac{i\hat{p}}{p^2 - m^2 + i0}, \quad \frac{-ig_{\mu\nu}}{k^2 - M^2 + i0}, \quad (\text{A1})$$

where p and k are the lepton and boson momenta, and m and M are the lepton and boson masses, respectively. We use the t'Hooft–Feynman gauge $\xi = 1$. The vector-lepton vertices are given by:

$$\begin{aligned} V(W^\mu, \nu_e, e_-) &= \frac{ie}{\sqrt{2}s_W} \gamma^\mu \omega_-; \\ V(Z^\mu, e, e) &= \frac{ie}{4s_W c_W} \gamma^\mu (-a_V - \gamma_5); \\ V(Z^\mu, \nu_e, \nu_e) &= \frac{ie}{2s_W c_W} \gamma^\mu \omega_-; \\ V(\gamma^\mu, e, e) &= -ie\gamma^\mu, \end{aligned}$$

where

$$a_V = 1 - 4s_W^2, \quad s_W = \sin \theta_W, \quad c_W = \cos \theta_W, \quad M_W = c_W M_Z,$$

and θ_W is the Weinberg angle.

Appendix B: lepton vertex functions

Let us calculate the correction to the electron vertex function coming from the Z -boson exchange (Fig. 5(b), 5(d)). Using the Feynman rules, we obtain:

$$\begin{aligned}\Gamma_\mu^Z \omega_\pm &= -ie\gamma_\mu \omega_\pm \frac{g^2(-a_V \mp 1)^2}{256\pi^2 c_W^2} I_Z, \\ I_Z &= \int \frac{d^4 k}{i\pi^2} \frac{N_Z}{(k^2 - M_Z^2)(k^2 - 2p_1 k)(k^2 - 2p'_1 k)}, \\ N_Z &= \gamma_\lambda (\hat{p}'_1 - \hat{k}) \gamma_\mu (\hat{p} - \hat{k}) \gamma^\lambda.\end{aligned}\tag{B1}$$

which leads to

$$I_Z = \int_0^1 dx \int_0^1 2y dy \left\{ \left(\ln \left(\frac{\Lambda^2}{d} \right) - \frac{3}{2} \right) - \frac{t}{2d} (1-yx)(1-y\bar{x}) \right\},\tag{B2}$$

where $d = y^2 p_x^2 + M_Z^2 \bar{y}$ and Λ is the ultraviolet cut-off parameter. To regularize this expression, we subtract from it the same expression but with $t = 0$.

The contribution from W^- exchange, $\Gamma_\mu^W \omega_+ = 0$ (Fig. 5(e)), is calculated in a similar way:

$$\begin{aligned}\Gamma_\mu^W \omega_- &= ie \frac{g^2}{32\pi^2} I_\mu^W, \\ I_\mu^W &= \int \frac{d^4 k}{i\pi^2} \frac{N_{W\mu}}{k^2(k^2 - 2p_1 k - M_W^2)(k^2 - 2p'_1 k - M_W^2)}, \\ N_{W\mu} &= \gamma^\nu \hat{k} \gamma^\lambda \omega_- [(p'_1 - 2p_1 + k)^\lambda g_{\mu\nu} + (p'_1 + p_1 - 2k)_\mu g_{\nu\lambda} + (p_1 - 2p'_1 + k)_\nu g_{\mu\lambda}].\end{aligned}$$

so we have

$$I_{W\mu} = \gamma_\mu \omega_- \int_0^1 dx \int_0^1 2y dy \left[3 \left(\ln \left(\frac{\Lambda^2}{D} \right) - \frac{3}{2} \right) + \frac{t}{2D} (2y^2 x(1-x) + y) \right],\tag{B3}$$

where $D = y^2 p_x^2 + y M_W^2$ and $p_x^2 = m^2 - x(1-x)t$.

Let us consider the case of a small momentum transfer: $-t = 2p_1 p'_1 \ll M_W^2$. Then, the result can be summarized in the form

$$\Gamma_\mu \omega_\pm = -ie\gamma_\mu \omega_\pm [1 + \Delta\Gamma_\pm^Z + \Delta\Gamma_\pm^W],\tag{B4}$$

where

$$\begin{aligned}\Delta\Gamma_+^W &= 0; \\ \Delta\Gamma_-^W &= \frac{17}{18} \frac{g^2}{32\pi^2} \frac{t}{M_W^2}, \quad -t \ll M_W^2; \\ \Delta\Gamma_\pm^Z &= \frac{g^2}{256\pi^2 c_W^2} \frac{-t}{M_W^2} (-a_V \mp 1)^2 \left(\frac{1}{6} \ln \frac{M_Z^2}{-t} + \frac{17}{36} \right).\end{aligned}$$

The contributions to the matrix element squared for a definite chiral state

$$\Delta_i^\lambda = 2\mathcal{M}_i^\lambda (\mathcal{M}_B^\lambda)^*\tag{B5}$$

are

$$\begin{aligned}\Delta_\Gamma^{++++} &= -\frac{16s^3(4\pi\alpha)^2}{tu} \left[\frac{\Delta\Gamma_Z(t)}{t} + \frac{\Delta\Gamma_Z(u)}{u} \right], \\ \Delta_\Gamma^{----} &= -\frac{16s^3(4\pi\alpha)^2}{tu} \left[\frac{\Delta\Gamma_Z(t) + \Delta\Gamma_W(t)}{t} + \frac{\Delta\Gamma_Z(u) + \Delta\Gamma_W(u)}{u} \right].\end{aligned}\tag{B6}$$

Appendix C: Contribution of W , Z to the vertex functions of the lepton, self-energy, and vacuum polarization

The contributions of WW and the relevant ghost intermediate states to the photon Green function (the vacuum-polarization operator) have a form (with $\xi = 1$):

$$\begin{aligned} \Pi_{\mu\nu} = & -\frac{ie^2 N}{32\pi^2(q^2)^2} \int \frac{dk}{(k^2 - M^2)((q-k)^2 - M^2)} \times \\ & \times [g_{\mu\nu}(2k^2 - 2kq + 5q^2) - 2q_\mu q_\nu + 10k_\mu k_\nu - 5(k_\mu q_\nu + k_\nu q_\mu)] + \\ & + \frac{ie^2 N}{16\pi^2(q^2)^2} \int \frac{dk}{(k^2 - M^2)((q-k)^2 - M^2)} k_\mu (q-k)_\nu, \end{aligned} \quad (C1)$$

where $M = M_W$, $N = 2$, $dk = d^4k/(i\pi^2)$. Using the set of divergent integrals [19],

$$\begin{aligned} \int \frac{dk}{AB} &= L - 1 - l, \quad A = k^2 - m^2, \quad L = \ln \frac{\Lambda^2}{m^2}, \\ \int \frac{dkk_\mu}{AB} &= \frac{1}{2} \left(L - l - \frac{3}{2} \right); \quad l = \int_0^1 \ln(1 - zx(1-x)), \quad z = \frac{q^2}{m^2}; \\ \int \frac{dkk_\mu k_\nu}{AB} &= g_{\mu\nu} \left[-\frac{1}{4}\Lambda^2 + \left(-\frac{1}{12}q^2 + \frac{1}{2}m^2 \right) L + \left(\frac{1}{12}q^2 - \frac{1}{3}m^2 \right) l + \frac{1}{72}q^2 - \frac{1}{4}m^2 \right] + \\ & + q_\mu q_\nu \left[\frac{1}{3}L + \left(\frac{1}{3}\frac{m^2}{q^2} - \frac{1}{3} \right) l - \frac{5}{9} \right], \end{aligned} \quad (C2)$$

where Λ is the ultraviolet cut-off parameter, we obtain

$$\begin{aligned} \Pi_{\mu\nu}(q) = & \frac{i\alpha}{4\pi} \left[g_{\mu\nu} \left[-4\Lambda^2 + \left(-\frac{10}{3}q^2 - \frac{14}{3}m^2 \right) l + \left(\frac{10}{3}q^2 + 8m^2 \right) L - 4m^2 - \frac{79}{18}q^2 \right] + \right. \\ & \left. + q_\mu q_\nu \left[-\frac{10}{3}L + \left(\frac{10}{3} + 8\frac{m^2}{q^2} \right) l + \frac{32}{9} \right] \right]. \end{aligned} \quad (C3)$$

After the regularization, we have

$$\Pi_{\mu\nu}(q) = \frac{i\alpha}{4\pi} \Pi \left(\frac{q^2}{m^2} \right) (q^2 g_{\mu\nu} - q_\nu q_\mu) + q_\mu q_\nu \Pi^l \left(\frac{q^2}{m^2} \right), \quad (C4)$$

where

$$\Pi(z) = \Pi^{SM}(z) = \left(-\frac{10}{3} + \frac{14}{3} \frac{1}{z} \right) \int_0^1 \ln(1 - zx(1-x)) dx - \frac{7}{9}. \quad (C5)$$

The term $\Pi^l(z)$ is irrelevant in our case. Let us consider the following important limiting cases:

$$\begin{aligned} \Pi^{SM}(z) &\approx -\frac{10}{3} \ln|z| + \frac{53}{9}, \quad -z \gg 1, \\ \Pi^{SM}(z) &\approx -\frac{19}{30}z + O(z^2), \quad |z| \ll 1. \end{aligned}$$

The ultraviolet behavior is in agreement with the phenomenon of asymptotic freedom in $SU(2)$. In our case, we use the non-relativistic limit $m = M_{W,Z}$. For the sake of completeness, we add the contribution of leptons calculated in the frame of QED:

$$\Pi^{QED}(z) = \frac{i\alpha}{3\pi} \left[\frac{1}{3} + \left(1 + \frac{2}{z} \right) \int_0^1 \ln(1 - zx(1-x)) dx \right]. \quad (C6)$$

with the limiting cases

$$\begin{aligned} \Pi^{QED}(z) &= \frac{i\alpha}{3\pi} \left(\ln|z| - \frac{5}{9} \right), \quad -z \gg 1, \\ \Pi^{QED}(z) &= \frac{-i\alpha}{15\pi} z, \quad |z| \ll 1. \end{aligned} \quad (C7)$$

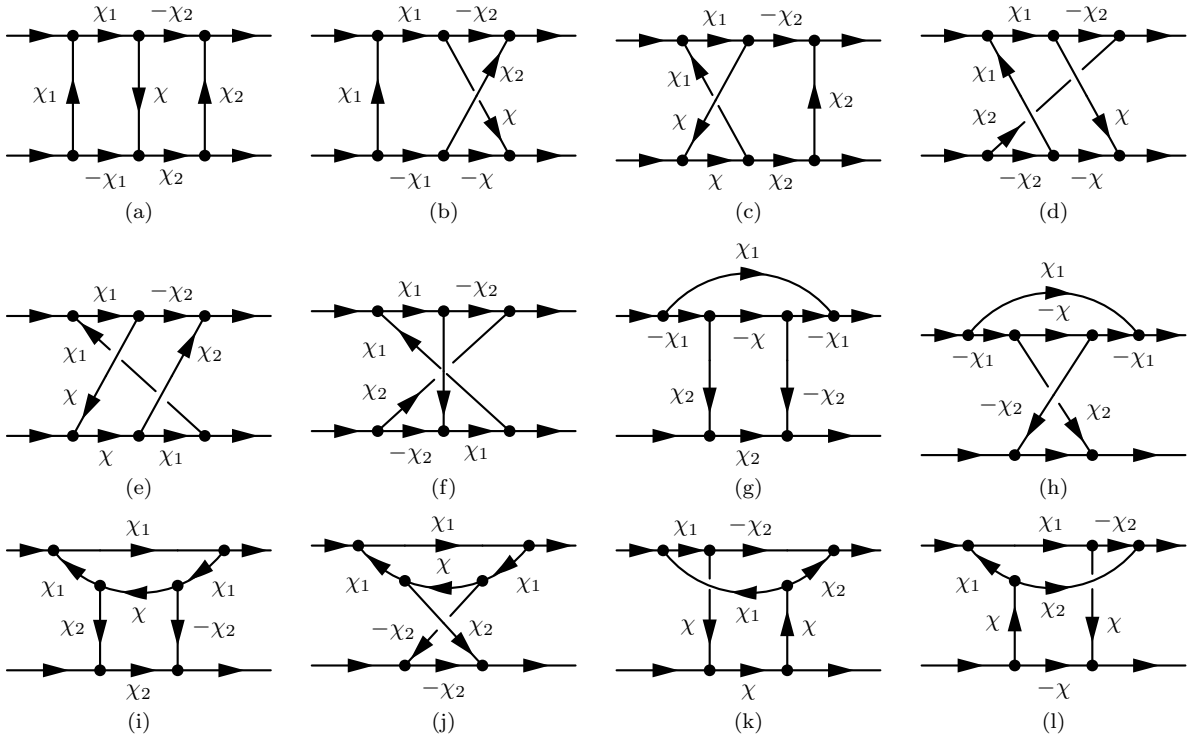


Figure 15: Two-loop topology diagrams.

Appendix D: Two-loop topologies and traces

Here we present the traces which correspond to the topologically-different diagrams shown in Fig. 15. Let's keep in mind that the momentum integration to be done after calculating the traces neglects the dependence on the external momenta. Thus, to simplify the expressions for the traces, we can average over momenta directions by using the following formulae:

$$\begin{aligned}
 \overline{\chi^\mu \chi^\nu \chi^\lambda \chi^\sigma} &= \frac{1}{24} (\chi^2)^2 G^{\mu\nu\lambda\sigma}, & \overline{\chi_{1,2}^\mu \chi_{1,2}^\nu \chi_{1,2}^\lambda \chi_{1,2}^\sigma} &= \frac{1}{24} (\chi_{1,2}^2)^2 G^{\mu\nu\lambda\sigma}, \\
 \overline{\chi_1^\mu \chi_1^\nu \chi_1^\lambda \chi_2^\sigma} &= \frac{1}{24} \alpha G^{\mu\nu\lambda\sigma}, & \overline{\chi^\mu \chi^\nu \chi^\lambda \chi_1^\sigma} &= \frac{1}{24} \tilde{\alpha} G^{\mu\nu\lambda\sigma}, \\
 \overline{\chi_2^\mu \chi_2^\nu \chi_2^\lambda \chi_1^\sigma} &= \frac{1}{24} \beta G^{\mu\nu\lambda\sigma}, & \overline{\chi_1^\mu \chi_1^\nu \chi_1^\lambda \chi^\sigma} &= \frac{1}{24} \tilde{\beta} G^{\mu\nu\lambda\sigma}, \\
 \overline{\chi_1^\mu \chi_1^\nu \chi_2^\lambda \chi_2^\sigma} &= a g^{\mu\nu} g^{\lambda\sigma} + b (g^{\mu\lambda} g^{\nu\sigma} + g^{\mu\sigma} g^{\nu\lambda}), & \overline{\chi^\mu \chi^\nu \chi_1^\lambda \chi_1^\sigma} &= \tilde{a} g^{\mu\nu} g^{\lambda\sigma} + \tilde{b} (g^{\mu\lambda} g^{\nu\sigma} + g^{\mu\sigma} g^{\nu\lambda}),
 \end{aligned}$$

where $\chi = \chi_1 + \chi_2$ and

$$\begin{aligned}
 G^{\mu\nu\lambda\sigma} &= g^{\mu\nu} g^{\lambda\sigma} + g^{\mu\lambda} g^{\nu\sigma} + g^{\mu\sigma} g^{\nu\lambda}, \\
 a &= \frac{1}{72} (5\gamma - 2\delta), & \tilde{a} &= \frac{1}{72} (5\tilde{\gamma} - 2\tilde{\delta}), \\
 b &= \frac{1}{72} (-\gamma + 4\delta), & \tilde{b} &= \frac{1}{72} (-\tilde{\gamma} + 4\tilde{\delta}),
 \end{aligned} \tag{D1}$$

and

$$\alpha = \chi_1^2 (\chi_1 \chi_2), \quad \beta = \chi_2^2 (\chi_1 \chi_2), \quad \gamma = \chi_1^2 \chi_2^2, \quad \delta = (\chi_1 \chi_2)^2, \tag{D2}$$

$$\tilde{\alpha} = \chi^2 (\chi \chi_1), \quad \tilde{\beta} = \chi_1^2 (\chi \chi_1), \quad \tilde{\gamma} = \chi^2 \chi_1^2, \quad \tilde{\delta} = (\chi \chi_1)^2. \tag{D3}$$

The traces then read as:

$$\text{Fig. 15(a)} : \quad S_{123} = \frac{1}{s^2 t} \text{Sp} [\hat{p}'_1 \gamma_\mu (-\hat{\chi}_2) \gamma_\nu \hat{\chi}_1 \gamma_\alpha \hat{p}_1 \hat{p}_2 \hat{p}'_2 \gamma^\mu \hat{\chi}_2 \gamma^\nu (-\hat{\chi}_1) \gamma^\alpha \hat{p}_2 \hat{p}_1 \omega_+] = 32\gamma, \quad (\text{D4})$$

$$\begin{aligned} \text{Fig. 15(b)} : \quad S_{213} &= \frac{1}{s^2 t} \text{Sp} [\hat{p}'_1 \gamma_\mu (-\hat{\chi}_2) \gamma_\nu \hat{\chi}_1 \gamma_\alpha \hat{p}_1 \hat{p}_2 \hat{p}'_2 \gamma^\nu (-\hat{\chi}_1) \gamma^\mu (-\hat{\chi}_1) \gamma^\alpha \hat{p}_2 \hat{p}_1 \omega_+] = \\ &= -8(\alpha + \gamma) = 8(\tilde{\beta} - \tilde{\gamma}), \end{aligned} \quad (\text{D5})$$

$$\begin{aligned} \text{Fig. 15(c)} : \quad S_{132} &= \frac{1}{s^2 t} \text{Sp} [\hat{p}'_1 \gamma_\mu (-\hat{\chi}_2) \gamma_\nu \hat{\chi}_1 \gamma_\alpha \hat{p}_1 \hat{p}_2 \hat{p}'_2 \gamma^\mu \hat{\chi}_2 \gamma^\alpha \hat{\chi}_1 \gamma^\nu \hat{p}_2 \hat{p}_1 \omega_+] = \\ &= -8(\beta + \gamma) = -8(\tilde{\alpha} + \tilde{\beta} - 2\tilde{\delta}), \end{aligned} \quad (\text{D6})$$

$$\begin{aligned} \text{Fig. 15(d)} : \quad S_{231} &= \frac{1}{s^2 t} \text{Sp} [\hat{p}'_1 \gamma_\mu (-\hat{\chi}_2) \gamma_\nu \hat{\chi}_1 \gamma_\alpha \hat{p}_1 \hat{p}_2 \hat{p}'_2 \gamma^\nu (-\hat{\chi}_1) \gamma^\alpha (-\hat{\chi}_2) \gamma^\mu \hat{p}_2 \hat{p}_1 \omega_+] = \\ &= -8(\beta + \gamma) = -8(\tilde{\alpha} + \tilde{\beta} - 2\tilde{\delta}), \end{aligned} \quad (\text{D7})$$

$$\begin{aligned} \text{Fig. 15(e)} : \quad S_{312} &= \frac{1}{s^2 t} \text{Sp} [\hat{p}'_1 \gamma_\mu (-\hat{\chi}_2) \gamma_\nu \hat{\chi}_1 \gamma_\alpha \hat{p}_1 \hat{p}_2 \hat{p}'_2 \gamma^\alpha \hat{\chi}_1 \gamma^\mu \hat{\chi}_1 \gamma^\nu \hat{p}_2 \hat{p}_1 \omega_+] = \\ &= -8(\alpha + \gamma) = 8(\tilde{\beta} - \tilde{\gamma}), \end{aligned} \quad (\text{D8})$$

$$\text{Fig. 15(f)} : \quad S_{321} = \frac{1}{s^2 t} \text{Sp} [\hat{p}'_1 \gamma_\mu (-\hat{\chi}_2) \gamma_\nu \hat{\chi}_1 \gamma_\alpha \hat{p}_1 \hat{p}_2 \hat{p}'_2 \gamma^\alpha \hat{\chi}_1 \gamma^\nu (-\hat{\chi}_2) \gamma^\mu \hat{p}_2 \hat{p}_1 \omega_+] = 8\delta, \quad (\text{D9})$$

$$\begin{aligned} \text{Fig. 15(g)} : \quad S_1^I &= \frac{1}{s^2 t} \text{Sp} [\hat{p}'_1 \gamma_\mu (-\hat{\chi}_1) \gamma_\nu (-\hat{\chi}_1) \gamma_\alpha (-\hat{\chi}_1) \gamma^\mu \hat{p}_1 \hat{p}_2 \hat{p}'_2 \gamma^\nu \hat{\chi}_2 \gamma^\alpha \hat{p}_2 \hat{p}_1 \omega_+] = \\ &= -8(\alpha + \gamma) = 8(\tilde{\beta} - \tilde{\gamma}), \end{aligned} \quad (\text{D10})$$

$$\begin{aligned} \text{Fig. 15(h)} : \quad S_2^I &= \frac{1}{s^2 t} \text{Sp} [\hat{p}'_1 \gamma_\mu (-\hat{\chi}_1) \gamma_\nu (-\hat{\chi}_1) \gamma_\alpha (-\hat{\chi}_1) \gamma^\mu \hat{p}_1 \hat{p}_2 \hat{p}'_2 \gamma^\alpha (-\hat{\chi}_2) \gamma^\nu \hat{p}_2 \hat{p}_1 \omega_+] = \\ &= -4(\alpha - \gamma + 2\delta) = 4(\tilde{\beta} + \tilde{\gamma} - 2\tilde{\delta}), \end{aligned} \quad (\text{D11})$$

$$\begin{aligned} \text{Fig. 15(i)} : \quad S_1^{II} &= \frac{1}{s^2 t} \text{Sp} [\hat{p}'_1 \gamma_\mu \hat{\chi}_1 \gamma_\nu \hat{p}_1 \hat{p}_2 \hat{p}'_2 \gamma_\alpha \hat{\chi}_2 \gamma_\beta \hat{p}_2 \hat{p}_1 \omega_+] V^{\mu\delta\alpha}(\chi_1, -\chi, \chi_2) V^{\nu\beta}_\delta(-\chi_1, -\chi_2, \chi) = \\ &= -9(\alpha + \beta + 4\gamma), \end{aligned} \quad (\text{D12})$$

$$\begin{aligned} \text{Fig. 15(i)} : \quad S_2^{II} &= \frac{1}{s^2 t} \text{Sp} [\hat{p}'_1 \gamma_\mu \hat{\chi}_1 \gamma_\nu \hat{p}_1 \hat{p}_2 \hat{p}'_2 \gamma_\alpha (-\hat{\chi}_2) \gamma_\beta \hat{p}_2 \hat{p}_1 \omega_+] V^{\mu\delta\beta}(\chi_1, -\chi, \chi_2) V^{\nu\alpha}_\delta(-\chi_1, -\chi_2, \chi) = \\ &= 15\alpha + 15\beta + 4\gamma + 20\delta, \end{aligned} \quad (\text{D13})$$

$$\begin{aligned} \text{Fig. 15(k)} : \quad S_1^{III} &= \frac{1}{s^2 t} \text{Sp} [\hat{p}'_1 \gamma_\mu (-\hat{\chi}_2) \gamma_\nu \hat{\chi}_1 \gamma_\alpha \hat{p}_1 \hat{p}_2 \hat{p}'_2 \gamma_\beta \hat{\chi}_1 \gamma^\nu \hat{p}_2 \hat{p}_1 \omega_+] V^{\mu\alpha\beta}(-\chi_2, -\chi_1, \chi) = \\ &= -6(\alpha + 2\beta + \gamma + 2\delta) = -6(2\tilde{\alpha} + \tilde{\beta} - \tilde{\gamma} - 2\tilde{\delta}), \end{aligned} \quad (\text{D14})$$

$$\begin{aligned} \text{Fig. 15(l)} : \quad S_2^{III} &= \frac{1}{s^2 t} \text{Sp} [\hat{p}'_1 \gamma_\mu (-\hat{\chi}_2) \gamma_\nu \hat{\chi}_1 \gamma_\alpha \hat{p}_1 \hat{p}_2 \hat{p}'_2 \gamma^\nu (-\hat{\chi}_1) \gamma_\beta \hat{p}_2 \hat{p}_1 \omega_+] V^{\mu\alpha\beta}(-\chi_2, -\chi_1, \chi) = \\ &= -6(2\alpha + \beta + \gamma + 2\delta) = -6(\tilde{\alpha} - \tilde{\beta}), \end{aligned} \quad (\text{D15})$$

where the three-boson vertex $V^{\mu\nu\alpha}$ is defined for incoming momenta as the following:

$$V^{\mu\nu\alpha}(k_1, k_2, k_3) = (k_2 - k_3)^\mu g^{\nu\alpha} + (k_3 - k_1)^\nu g^{\mu\alpha} + (k_1 - k_2)^\alpha g^{\mu\nu}. \quad (\text{D16})$$

We should also evaluate the trace for the diagram of $WW\gamma$ exchange (see Fig. 10):

$$\begin{aligned} S_{WW\gamma} &= \frac{1}{s^2 t} \text{Sp} [\hat{p}'_1 \gamma_\mu (-\hat{\chi}_1) \gamma_\nu \hat{p}_1 \hat{p}_2 \hat{p}'_2 \gamma_\alpha (-\hat{\chi}_1) \gamma_\beta \hat{p}_2 \hat{p}_1 \omega_+] V^{\mu\beta}_\rho(\chi, -\chi_1, -\chi_2) V^{\alpha\rho\nu}(-\chi, \chi_2, \chi_1) = \\ &= 2(6\tilde{\alpha} + 6\tilde{\beta} - 7\tilde{\gamma} - 8\tilde{\delta}). \end{aligned} \quad (\text{D17})$$

Appendix E: Integration over the two-loop momenta

In this section we present a set of loop integrals used to evaluate the two-loop contributions. Although the loop momenta are normally denoted as χ_1 and χ_2 , sometimes it is more convenient to use another set of variables, $\chi = \chi_1 + \chi_2$

and χ_1 . A convenient way to classify the loop integrals is by the construction of the momenta in the numerators (see (D2) and (D3)). For the loop integral denominators, we use the following notation:

$$\mathbf{a} = \chi_1^2, \quad \mathbf{a}_Z = \mathbf{a} + M_Z^2, \quad \mathbf{a}_W = \mathbf{a} + M_W^2, \quad \mathbf{a}_e = \mathbf{a} + m^2, \quad (\text{E1})$$

$$\mathbf{b} = \chi_2^2, \quad \mathbf{b}_Z = \mathbf{b} + M_Z^2, \quad \mathbf{b}_W = \mathbf{b} + M_W^2, \quad \mathbf{b}_e = \mathbf{b} + m^2, \quad (\text{E2})$$

$$\mathbf{c} = \chi^2, \quad \mathbf{c}_Z = \mathbf{c} + M_Z^2, \quad \mathbf{c}_W = \mathbf{c} + M_W^2, \quad \mathbf{c}_e = \mathbf{c} + m^2.$$

Below we present the full set of master integrals used for the two-loop integration:

$$M_Z^2 \int \frac{d\chi_1 d\chi_2 \gamma}{\mathbf{a}_e^2 \mathbf{b}_e^2 \mathbf{a}_Z \mathbf{b}_Z \mathbf{c}_Z} = - \int_0^1 dy \int_0^1 dx \int_0^\infty dz \frac{\bar{x}}{(z+1)(\alpha + \beta z)} = -1.87093,$$

$$M_Z^2 \int \frac{d\chi_1 d\chi_2 \alpha}{\mathbf{a}_e^2 \mathbf{b}_e \mathbf{c}_e \mathbf{a}_Z \mathbf{b}_Z \mathbf{c}_Z} = M_Z^2 \int \frac{d\chi_1 d\chi_2 \beta}{\mathbf{a}_e \mathbf{b}_e^2 \mathbf{c}_e \mathbf{a}_Z \mathbf{b}_Z \mathbf{c}_Z} = - \int_0^1 dy \int_0^1 dx \int_0^\infty dz \frac{x^2 \bar{x} z}{(z+1)(\alpha + \beta z)^2} = -0.210286,$$

$$M_Z^2 \int \frac{d\chi_1 d\chi_2 \gamma}{\mathbf{a}_e^2 \mathbf{b}_e \mathbf{c}_e \mathbf{a}_Z \mathbf{b}_Z \mathbf{c}_Z} = M_Z^2 \int \frac{d\chi_1 d\chi_2 \gamma}{\mathbf{a}_e \mathbf{b}_e^2 \mathbf{c}_e \mathbf{a}_Z \mathbf{b}_Z \mathbf{c}_Z} = - \int_0^1 dy \int_0^1 dx \int_0^\infty dz \frac{x}{(z+1)(\alpha_y + \beta z)^2} = -1.87093,$$

$$M_Z^2 \int \frac{d\chi_1 d\chi_2 \delta}{\mathbf{a}_e^2 \mathbf{b}_e^2 \mathbf{a}_Z \mathbf{b}_Z \mathbf{c}_Z} = - \int_0^1 dy \int_0^1 dx \int_0^\infty dz \bar{y} \bar{x}^2 \left(\frac{1}{2} \frac{1}{(z+1)(\alpha + \beta z)} + x^2 \frac{z}{(z+1)(\alpha + \beta z)^2} \right) = -0.540199,$$

$$M_Z^2 \int \frac{d\chi_1 d\chi_2 \alpha}{\mathbf{a}_e^2 \mathbf{b}_e \mathbf{c}_e \mathbf{a}_Z \mathbf{b}_Z \mathbf{c}_Z} = \int_0^1 dt \int_0^1 dy \int_0^1 dx \frac{x}{\bar{x}y + xt} = 1.64493,$$

$$M_Z^2 \int \frac{d\chi_1 d\chi_2 \gamma}{\mathbf{a}_e^2 \mathbf{b}_e \mathbf{c}_e \mathbf{a}_Z \mathbf{b}_Z \mathbf{c}_Z} = - \int_0^1 dt \int_0^1 dy \int_0^1 dx \frac{1}{\bar{x}y + xt} = -2\zeta_2 = -3.28987,$$

$$M_Z^2 \int \frac{d\chi d\chi_1 \tilde{\alpha}}{\mathbf{a}_e^2 \mathbf{b}_e \mathbf{c}_e \mathbf{a}_Z \mathbf{b}_Z \mathbf{c}} = - \int_0^1 dt \int_0^1 dy \int_0^1 dx \frac{y}{\bar{x}y + xt} = -1.14493,$$

$$M_Z^2 \int \frac{d\chi d\chi_1 \tilde{\beta}}{\mathbf{a}_e^2 \mathbf{b}_e \mathbf{c}_e \mathbf{a}_Z \mathbf{b}_Z \mathbf{c}} = \int_0^1 dt \int_0^1 dy \int_0^1 dx \frac{x}{\bar{x}y + xt} = 1.64493,$$

$$M_Z^2 \int \frac{d\chi d\chi_1 \tilde{\gamma}}{\mathbf{a}_e^2 \mathbf{b}_e \mathbf{c}_e \mathbf{a}_Z \mathbf{b}_Z \mathbf{c}} = - \int_0^1 dt \int_0^1 dy \int_0^1 dx \frac{1}{\bar{x}y + xt} = -3.28987,$$

$$M_Z^2 \int \frac{d\chi_1 d\chi_2 \beta}{\mathbf{a}_e \mathbf{b}_e^2 \mathbf{c}_e \mathbf{a}_Z \mathbf{b}_Z} = \frac{1}{2} L_Z + \int_0^1 dy \int_0^1 dx \bar{x} \ln \left(\frac{\bar{x}y(x + \bar{x}y)}{\beta^2} \right) \ln \left(\frac{x + \bar{x}y}{\bar{x}y} \right) - \int_0^1 dt \int_0^1 dy \int_0^1 dx \frac{x \bar{x}}{\bar{x}y + xt} = \frac{1}{2} L_Z - 0.289868,$$

$$M_Z^2 \int \frac{d\chi_1 d\chi_2 \gamma}{\mathbf{a}_e \mathbf{b}_e^2 \mathbf{c}_e \mathbf{a}_Z \mathbf{b}_Z} = -L_Z - \frac{1}{2} \int_0^1 dx \ln \left(\frac{x}{\beta^2} \right) \ln \left(\frac{1}{\bar{x}} \right) = -L_Z - 2.17753,$$

$$M_Z^2 \int \frac{d\chi_1 d\chi_2 \beta}{\mathbf{a} \mathbf{a}_e \mathbf{b}_e^2 \mathbf{c}_e \mathbf{b}_Z \mathbf{c}_Z} = \int_0^1 dy \int_0^1 dx \ln \left(\frac{x + y \bar{x}}{y \bar{x}} \right) = 1.64493,$$

$$M_Z^2 \int \frac{d\chi_1 d\chi_2 \gamma}{\mathbf{a} \mathbf{a}_e \mathbf{b}_e^2 \mathbf{c}_e \mathbf{b}_Z \mathbf{c}_Z} = - \int_0^1 dy \int_0^1 dx \int_0^\infty dz \frac{1}{(z+1)(y + zx)} = -2\zeta_2 = -3.28987,$$

$$\begin{aligned}
M_Z^2 \int \frac{d\chi_1 d\chi_2 \gamma}{\mathbf{a}_e^2 \mathbf{b}_e^2 \mathbf{c}_A \mathbf{z} \mathbf{b}_Z} &= - \int_0^1 dy \int_0^1 dx \int_0^\infty dz \frac{1}{(z+1)(y+zx)} = -2\zeta_2 = -3.28987, \\
M_Z^2 \int \frac{d\chi_1 d\chi_2 \delta}{\mathbf{a}_e^2 \mathbf{b}_e^2 \mathbf{c}_A \mathbf{z} \mathbf{b}_Z} &= - \int_0^1 dy \int_0^1 dx \int_0^\infty dz y \left(\frac{\bar{x}}{2} \frac{1}{(z+1)(y+zx)} + x^2 \frac{z}{(z+1)(y+zx)^2} \right) = -0.572467, \\
M_Z^2 \int \frac{d\chi d\chi_1 \tilde{\alpha}}{\mathbf{a}_e \mathbf{b} \mathbf{c}_e \mathbf{a}_W^2 \mathbf{c}_W^2} &= - \int_0^1 dy \int_0^1 dx \int_0^\infty dz \frac{yxz^2}{(z+1)^2 (y+zx)^2} = -0.355066, \\
M_Z^2 \int \frac{d\chi d\chi_1 \tilde{\beta}}{\mathbf{a}_e \mathbf{b} \mathbf{c}_e \mathbf{a}_W^2 \mathbf{c}_W^2} &= - \int_0^1 dx \int_0^\infty dz \frac{xz}{(z+1)^2 (1+zx)} = -0.355066, \\
M_Z^2 \int \frac{d\chi d\chi_1 \tilde{\gamma}}{\mathbf{a}_e \mathbf{b} \mathbf{c}_e \mathbf{a}_W^2 \mathbf{c}_W^2} &= - \int_0^1 dx \int_0^\infty dz \frac{z}{(z+1)^2 (1+zx)} = -1, \\
M_Z^2 \int \frac{d\chi d\chi_1 \tilde{\delta}}{\mathbf{a}_e \mathbf{b} \mathbf{c}_e \mathbf{a}_W^2 \mathbf{c}_W^2} &= - \int_0^1 dy \int_0^1 dx \int_0^\infty dz y \left(\frac{\bar{x}}{2} \frac{z}{(z+1)^2 (y+zx)} + x^2 \frac{z^2}{(z+1)^2 (y+zx)^2} \right) = -0.355066, \\
M_Z^2 \int \frac{d\chi_1 d\chi_2 \beta}{\mathbf{a} \mathbf{b}_e^2 \mathbf{c}_A \mathbf{a}_W \mathbf{b}_Z \mathbf{c}_W} &= M_Z^2 \int \frac{d\chi_1 d\chi_2 \alpha}{\mathbf{a}_e^2 \mathbf{b} \mathbf{c}_A \mathbf{z} \mathbf{b}_W \mathbf{c}_W} = \int_0^1 dt \int_0^1 dy \int_0^1 dx \int_0^\infty dz \frac{x^2 \bar{x} z}{(z+1)(a_t c_W^2 + \beta z)^2} = 1.13521, \\
M_Z^2 \int \frac{d\chi_1 d\chi_2 \gamma}{\mathbf{a} \mathbf{b}_e^2 \mathbf{c}_A \mathbf{a}_W \mathbf{b}_Z \mathbf{c}_W} &= M_Z^2 \int \frac{d\chi_1 d\chi_2 \gamma}{\mathbf{a}_e^2 \mathbf{b} \mathbf{c}_A \mathbf{z} \mathbf{b}_W \mathbf{c}_W} = - \int_0^1 dt \int_0^1 dx \int_0^\infty dz \frac{x}{(z+1)(\alpha_t c_W^2 + \beta z)} = -2.20072, \\
M_Z^2 \int \frac{d\chi_1 d\chi_2 \alpha}{\mathbf{a}^2 \mathbf{b}_e \mathbf{c}_A \mathbf{a}_W \mathbf{b}_Z \mathbf{c}_W} &= M_Z^2 \int \frac{d\chi_1 d\chi_2 \beta}{\mathbf{a}_e \mathbf{b}^2 \mathbf{c}_A \mathbf{z} \mathbf{b}_W \mathbf{c}_W} = \int_0^1 dt \int_0^1 dy \int_0^1 dx \int_0^\infty dz \frac{x^2 \bar{x} z}{(z+1)(a_t c_W^2 + \beta z)^2} = 1.13521, \\
M_Z^2 \int \frac{d\chi_1 d\chi_2 \gamma}{\mathbf{a}^2 \mathbf{b}_e \mathbf{c}_A \mathbf{a}_W \mathbf{b}_Z \mathbf{c}_W} &= M_Z^2 \int \frac{d\chi_1 d\chi_2 \gamma}{\mathbf{a}_e \mathbf{b}^2 \mathbf{c}_A \mathbf{z} \mathbf{b}_W \mathbf{c}_W} = \int_0^1 dt \int_0^1 dy \int_0^1 dx \int_0^\infty dz \frac{x \bar{x} z}{(z+1)(a_t c_W^2 + \beta z)^2} = 2.27042, \\
M_Z^2 \int \frac{d\chi_1 d\chi_2 \alpha}{\mathbf{a}^2 \mathbf{b} \mathbf{c}_e \mathbf{a}_W \mathbf{b}_W \mathbf{c}_Z} &= M_Z^2 \int \frac{d\chi_1 d\chi_2 \beta}{\mathbf{a} \mathbf{b}^2 \mathbf{c}_e \mathbf{a}_W \mathbf{b}_W \mathbf{c}_Z} = \\
&= \int_0^1 dt \int_0^1 dy \int_0^1 dx \int_0^\infty dz \frac{x^2 \bar{x} z}{(z+c_W^2)(c_W^2 \bar{x} y + xt + \beta z)^2} = 1.06551, \\
M_Z^2 \int \frac{d\chi_1 d\chi_2 \gamma}{\mathbf{a}^2 \mathbf{b} \mathbf{c}_e \mathbf{a}_W \mathbf{b}_W \mathbf{c}_Z} &= M_Z^2 \int \frac{d\chi_1 d\chi_2 \gamma}{\mathbf{a} \mathbf{b}^2 \mathbf{c}_e \mathbf{a}_W \mathbf{b}_W \mathbf{c}_Z} = \\
&= - \int_0^1 dt \int_0^1 dy \int_0^1 dx \int_0^\infty dz \frac{x \bar{x} z}{(z+c_W^2)(c_W^2 \bar{x} y + xt + \beta z)^2} = -2.20072, \\
M_Z^2 \int \frac{d\chi_1 d\chi_2 \delta}{\mathbf{a}^2 \mathbf{b}^2 \mathbf{a}_W \mathbf{b}_W \mathbf{c}_Z} &= \\
&= - \int_0^1 dy \int_0^1 dx \int_0^\infty dz y \bar{x}^2 \left(\frac{1}{2} \frac{1}{(z+c_W^2)(c_W^2 \bar{x} y + x + \beta z)} + x^2 \frac{z}{(z+c_W^2)(c_W^2 \bar{x} y + x + \beta z)^2} \right) = -0.648595, \\
M_Z^2 \int \frac{d\chi_1 d\chi_2 \alpha}{\mathbf{a}_e^2 \mathbf{b}^2 \mathbf{b}_e \mathbf{c}_A \mathbf{z}} &= \frac{1}{4} L_Z^2 + \frac{1}{4} L_Z + \zeta_2 + \frac{1}{8}, \\
M_Z^2 \int \frac{d\chi_1 d\chi_2 \gamma}{\mathbf{a}_e^2 \mathbf{b}^2 \mathbf{b}_e \mathbf{c}_A \mathbf{z}} &= -\frac{1}{2} L_Z^2 - L_Z - 2\zeta_2 - \frac{1}{8},
\end{aligned}$$

$$\begin{aligned}
M_Z^2 \int \frac{d\chi_1 d\chi_2 \delta}{\mathbf{a}_e^2 \mathbf{b}^2 \mathbf{b}_e \mathbf{c}_e \mathbf{a}_Z} &= -\frac{1}{8}L_Z^2 - \frac{5}{8}L_Z - \frac{1}{2}\zeta_2 - \frac{1}{16}, \\
M_Z^2 \int \frac{d\chi_1 d\chi_2 \alpha}{\mathbf{a}_e^2 \mathbf{b}_e \mathbf{b} \mathbf{c}_e \mathbf{a}_Z \mathbf{b}_Z} &= \int_0^1 dy \int_0^1 dx \int_0^\infty dz \frac{x\bar{y}z}{(z+1)(y+zx)^2} = 1.14493, \\
M_Z^2 \int \frac{d\chi_1 d\chi_2 \gamma}{\mathbf{a}_e^2 \mathbf{b}_e \mathbf{b} \mathbf{c}_e \mathbf{a}_Z \mathbf{b}_Z} &= -\int_0^1 dy \int_0^1 dx \int_0^\infty dz \frac{1}{(z+1)(y+\bar{x}z)} = -3.28987, \\
M_Z^2 \int \frac{d\chi_1 d\chi_2 \delta}{\mathbf{a}_e^2 \mathbf{b}_e \mathbf{b} \mathbf{c}_e \mathbf{a}_Z \mathbf{b}_Z} &= -\int_0^1 dy \int_0^1 dx \int_0^\infty dz \bar{y} \left(\frac{\bar{x}}{2} \frac{1}{(z+1)(y+xz)} + x^2 \frac{z}{(z+1)(y+xz)^2} \right) = -1.14493, \\
M_Z^2 \int \frac{d\chi_1 d\chi_2 \alpha}{\mathbf{a}_e^2 \mathbf{b}_e \mathbf{c}_e \mathbf{a}_Z \mathbf{b}_Z^2} &= \int_0^1 dy \int_0^1 dx \int_0^\infty dz \frac{xz}{(z+1)^2 (y+xz)} = 0.5, \\
M_Z^2 \int \frac{d\chi_1 d\chi_2 \gamma}{\mathbf{a}_e^2 \mathbf{b}_e \mathbf{c}_e \mathbf{a}_Z \mathbf{b}_Z^2} &= -\int_0^1 dy \int_0^1 dx \int_0^\infty dz \frac{z}{(z+1)^2 (y+xz)} = -1.64493, \\
M_Z^2 \int \frac{d\chi_1 d\chi_2 \delta}{\mathbf{a}_e^2 \mathbf{b}_e \mathbf{c}_e \mathbf{a}_Z \mathbf{b}_Z^2} &= -\int_0^1 dy \int_0^1 dx \int_0^\infty dz \bar{y} \left(\frac{\bar{x}}{2} \frac{z}{(z+1)^2 (y+xz)} + x^2 \frac{z^2}{(z+1)^2 (y+xz)^2} \right) = -0.572467, \\
M_Z^2 \int \frac{d\chi_1 d\chi_2 \alpha}{\mathbf{a}^2 \mathbf{b}_e \mathbf{c} \mathbf{a}_W \mathbf{b}_Z^2} &= \int_0^1 dy \int_0^1 dx \int_0^\infty dz \frac{xz}{(z+1)^2 (yc_W^2 + xz)} = 0.538035, \\
M_Z^2 \int \frac{d\chi_1 d\chi_2 \gamma}{\mathbf{a}^2 \mathbf{b}_e \mathbf{c} \mathbf{a}_W \mathbf{b}_Z^2} &= -\int_0^1 dy \int_0^1 dx \int_0^\infty dz \frac{z}{(z+1)^2 (yc_W^2 + xz)} = -1.81942, \\
M_Z^2 \int \frac{d\chi_1 d\chi_2 \delta}{\mathbf{a}^2 \mathbf{b}_e \mathbf{c} \mathbf{a}_W \mathbf{b}_Z^2} &= -\int_0^1 dy \int_0^1 dx \int_0^\infty dz \bar{y} \left(\frac{\bar{x}}{2} \frac{z}{(z+1)^2 (yc_W^2 + xz)} + x^2 \frac{z^2}{(z+1)^2 (yc_W^2 + xz)^2} \right) = -0.630951, \\
M_Z^2 \int \frac{d\chi_1 d\chi_2 \alpha}{\mathbf{a}_e^2 \mathbf{b} \mathbf{c} \mathbf{a}_Z \mathbf{b}_W^2} &= \int_0^1 dy \int_0^1 dx \int_0^\infty dz \frac{1}{(z+c_W^2)^2 (y+xz)} = 2.36647, \\
M_Z^2 \int \frac{d\chi_1 d\chi_2 \gamma}{\mathbf{a}_e^2 \mathbf{b} \mathbf{c} \mathbf{a}_Z \mathbf{b}_W^2} &= -\int_0^1 dy \int_0^1 dx \int_0^\infty dz \frac{z}{(z+c_W^2)^2 (y+xz)} = -1.9256, \\
M_Z^2 \int \frac{d\chi_1 d\chi_2 \delta}{\mathbf{a}_e^2 \mathbf{b} \mathbf{c} \mathbf{a}_Z \mathbf{b}_W^2} &= -\int_0^1 dy \int_0^1 dx \int_0^\infty dz \bar{y} \left(\frac{\bar{x}}{2} \frac{z}{(z+c_W^2)^2 (y+xz)} + x^2 \frac{z^2}{(z+c_W^2)^2 (y+xz)^2} \right) = -0.672106, \\
M_Z^2 \int \frac{d\chi_1 d\chi_2 \alpha}{\mathbf{a} \mathbf{b}^2 \mathbf{b}_e \mathbf{a}_W^2 \mathbf{c}_W} &= \frac{1}{c_W^2} \left(\frac{1}{6}L_W + \frac{5}{18} \right), \\
M_Z^2 \int \frac{d\chi_1 d\chi_2 \beta}{\mathbf{a} \mathbf{b}^2 \mathbf{b}_e \mathbf{a}_W^2 \mathbf{c}_W} &= \int_0^1 dy \int_0^1 dx \frac{\bar{x}y}{x+\bar{x}y} = \frac{1}{c_W^2} 0.355066, \\
M_Z^2 \int \frac{d\chi_1 d\chi_2 \gamma}{\mathbf{a} \mathbf{b}^2 \mathbf{b}_e \mathbf{a}_W^2 \mathbf{c}_W} &= -\frac{1}{c_W^2} \left(\frac{1}{2}L_W + 1 \right), \\
M_Z^2 \int \frac{d\chi_1 d\chi_2 \delta}{\mathbf{a} \mathbf{b}^2 \mathbf{b}_e \mathbf{a}_W^2 \mathbf{c}_W} &= -\frac{1}{c_W^2} \left(\frac{1}{8}L_W - \frac{6}{8}\zeta_2 + \frac{13}{8} \right), \\
M_Z^2 \int \frac{d\chi_1 d\chi_2 \alpha}{\mathbf{a} \mathbf{b}_e \mathbf{a}_W^2 \mathbf{b} \mathbf{b}_Z \mathbf{c}_W} &= \int_0^1 dx \int_0^\infty dz \frac{x\bar{x}}{(z+1)(c_W^2 + \beta z)} = 0.405476,
\end{aligned}$$

$$\begin{aligned}
M_Z^2 \int \frac{d\chi_1 d\chi_2 \beta}{\mathbf{a} \mathbf{b}_e \mathbf{a}_W^2 \mathbf{b} \mathbf{b}_Z \mathbf{c}_W} &= \int_0^1 dx \int_0^1 dy \int_0^\infty dz \frac{x\bar{x}z}{(z+1)(c_W^2(x+\bar{x}y) + \beta z)^2} = 0.861218, \\
M_Z^2 \int \frac{d\chi_1 d\chi_2 \gamma}{\mathbf{a} \mathbf{b}_e \mathbf{a}_W^2 \mathbf{b} \mathbf{b}_Z \mathbf{c}_W} &= - \int_0^1 dx \int_0^\infty dz \frac{\bar{x}}{(z+1)(c_W^2 + \beta z)} = -1.39341, \\
M_Z^2 \int \frac{d\chi_1 d\chi_2 \delta}{\mathbf{a} \mathbf{b}_e \mathbf{a}_W^2 \mathbf{b} \mathbf{b}_Z \mathbf{c}_W} &= \\
&= - \int_0^1 dx \int_0^1 dy \int_0^\infty dz y \bar{x}^2 \left(\frac{1}{2(z+1)(c_W^2(x+\bar{x}y) + \beta z)} + x^2 \frac{z}{(z+1)(c_W^2(x+\bar{x}y) + \beta z)^2} \right) = -0.418052, \\
M_Z^2 \int \frac{d\chi_1 d\chi_2 \alpha}{\mathbf{a} \mathbf{b}_e \mathbf{a}_W^2 \mathbf{b}_Z^2 \mathbf{c}_W} &= \int_0^1 dx \int_0^\infty dz \frac{x\bar{x}z}{(z+1)^2(c_W^2 + \beta z)} = 0.250133, \\
M_Z^2 \int \frac{d\chi_1 d\chi_2 \beta}{\mathbf{a} \mathbf{b}_e \mathbf{a}_W^2 \mathbf{b}_Z^2 \mathbf{c}_W} &= \int_0^1 dx \int_0^1 dy \int_0^\infty dz \frac{yx\bar{x}^2 z^2}{(z+1)^2(c_W^2(x+\bar{x}y) + \beta z)^2} = 0.264515, \\
M_Z^2 \int \frac{d\chi_1 d\chi_2 \gamma}{\mathbf{a} \mathbf{b}_e \mathbf{a}_W^2 \mathbf{b}_Z^2 \mathbf{c}_W} &= - \int_0^1 dx \int_0^\infty dz \frac{\bar{x}z}{(z+1)^2(1 + \beta z)} = -0.781303, \\
M_Z^2 \int \frac{d\chi_1 d\chi_2 \delta}{\mathbf{a} \mathbf{b}_e \mathbf{a}_W^2 \mathbf{b}_Z^2 \mathbf{c}_W} &= \\
&= - \int_0^1 dx \int_0^1 dy \int_0^\infty dz y \bar{x}^2 \left(\frac{1}{2(z+1)^2(c_W^2(x+y\bar{x}) + \beta z)} + x^2 \frac{z^2}{(z+1)^2(c_W^2(x+y\bar{x}) + \beta z)^2} \right) = -0.281296, \\
M_Z^2 \int \frac{d\chi_1 d\chi_2 \alpha}{\mathbf{a}_e \mathbf{b} \mathbf{a}_Z^2 \mathbf{b}_W^2 \mathbf{c}_W} &= \int_0^1 dx \int_0^1 dy \int_0^\infty dz \frac{x\bar{x}^2 z^2}{(z+1)^2(c_W^2(x+\bar{x}y) + \beta z)^2} = 0.674289, \\
M_Z^2 \int \frac{d\chi_1 d\chi_2 \beta}{\mathbf{a}_e \mathbf{b} \mathbf{a}_Z^2 \mathbf{b}_W^2 \mathbf{c}_W} &= \int_0^1 dx \int_0^\infty dz \frac{x\bar{x}z}{(z+1)^2(c_W^2 + \beta z)} = 0.250133, \\
M_Z^2 \int \frac{d\chi_1 d\chi_2 \gamma}{\mathbf{a}_e \mathbf{b} \mathbf{a}_Z^2 \mathbf{b}_W^2 \mathbf{c}_W} &= - \int_0^1 dx \int_0^\infty dz \frac{xz}{(z+1)^2(c_W^2 + \beta z)} = -0.905742, \\
M_Z^2 \int \frac{d\chi_1 d\chi_2 \delta}{\mathbf{a}_e \mathbf{b} \mathbf{a}_Z^2 \mathbf{b}_W^2 \mathbf{c}_W} &= \\
&= - \int_0^1 dx \int_0^1 dy \int_0^\infty dz y \bar{x}^2 \left(\frac{1}{2(z+1)^2(c_W^2(x+\bar{x}y) + \beta z)} + x^2 \frac{z^2}{(z+1)^2(c_W^2(x+\bar{x}y) + \beta z)^2} \right) = -0.281296, \\
M_Z^2 \int \frac{d\chi d\chi_1 \tilde{\alpha}}{\mathbf{a} \mathbf{b} \mathbf{c}_e \mathbf{a}_W \mathbf{b}_W \mathbf{c}_Z \mathbf{c}} &= - \int_0^1 dx \int_0^1 dy \int_0^1 dt \int_0^\infty dz \frac{x^2 \bar{x}z}{(z+1)(c_W^2(\bar{x}y + xt) + \beta z)^2} = -1.13521, \\
M_Z^2 \int \frac{d\chi d\chi_1 \tilde{\beta}}{\mathbf{a} \mathbf{b} \mathbf{c}_e \mathbf{a}_W \mathbf{b}_W \mathbf{c}_Z \mathbf{c}} &= - \int_0^1 dx \int_0^1 dy \int_0^\infty dz \frac{x^2}{(z+1)(c_W^2(\bar{x} + xy) + \beta z)} = -1.6915, \\
M_Z^2 \int \frac{d\chi d\chi_1 \tilde{\gamma}}{\mathbf{a} \mathbf{b} \mathbf{c}_e \mathbf{a}_W \mathbf{b}_W \mathbf{c}_Z \mathbf{c}} &= - \int_0^1 dx \int_0^1 dy \int_0^\infty dz \frac{x}{(z+1)(c_W^2(\bar{x} + xy) + \beta z)} = -2.20072, \\
M_Z^2 \int \frac{d\chi d\chi_1 \tilde{\delta}}{\mathbf{a} \mathbf{b} \mathbf{c}_e \mathbf{a}_W \mathbf{b}_W \mathbf{c}_Z \mathbf{c}} &=
\end{aligned}$$

$$\begin{aligned}
& - \int_0^1 dx \int_0^1 dy \int_0^1 dt \int_0^\infty dz x \bar{x} \left(\frac{1}{2} \frac{1}{(z+1)(c_W^2(\bar{x}y+xt)+\beta z)} + x^2 \frac{z}{(z+1)(c_W^2(\bar{x}y+xt)+\beta z)^2} \right) = -1.15873, \\
M_Z^2 \int \frac{d\chi_1 d\chi_2 \alpha}{\mathbf{a} \mathbf{b} \mathbf{c}_e \mathbf{a}_W \mathbf{b}_W \mathbf{c}_Z^2} &= M_Z^2 \int \frac{d\chi_1 d\chi_2 \beta}{\mathbf{a} \mathbf{b} \mathbf{c}_e \mathbf{a}_W \mathbf{b}_W \mathbf{c}_Z^2} = \\
&= -2 \int_0^1 dx \int_0^1 dy \int_0^1 dt \int_0^\infty dz \frac{tx^3 \bar{x} z}{(z+c_W^2)(c_W^2 \bar{x}y+xt+\beta z)^3} = -0.549109, \\
M_Z^2 \int \frac{d\chi_1 d\chi_2 \gamma}{\mathbf{a} \mathbf{b} \mathbf{c}_e \mathbf{a}_W \mathbf{b}_W \mathbf{c}_Z^2} &= - \int_0^1 dt \int_0^1 dx \int_0^\infty dz \frac{tx^2 z}{(z+c_W^2)(c_W^2 \bar{x}+xt+\beta z)^2} = -2.61154, \\
M_Z^2 \int \frac{d\chi_1 d\chi_2 \delta}{\mathbf{a} \mathbf{b} \mathbf{c}_e \mathbf{a}_W \mathbf{b}_W \mathbf{c}_Z^2} &= -2 \int_0^1 dt \int_0^1 dx \int_0^1 dy \int_0^\infty dz t \bar{x} x^2 \times \\
&\times \left(\frac{1}{4} \frac{z}{(z+c_W^2)(c_W^2 \bar{x}y+xt+\beta z)^2} + x^2 \frac{z^2}{(z+c_W^2)(c_W^2 \bar{x}y+xt+\beta z)^3} \right) = -2.96868, \\
M_Z^2 \int \frac{d\chi d\chi_1 \tilde{\alpha}}{\mathbf{a}_e \mathbf{b} \mathbf{c} \mathbf{a}_Z \mathbf{b}_W \mathbf{c}_W^2} &= - \int_0^1 dt \int_0^1 dx \int_0^1 dy \int_0^\infty dz \frac{x^2 \bar{x} z^2}{(z+c_W^2)^2 (c_W^2 xt + \bar{x}y + \beta z)^2} = -0.861218, \\
M_Z^2 \int \frac{d\chi d\chi_1 \tilde{\beta}}{\mathbf{a}_e \mathbf{b} \mathbf{c} \mathbf{a}_Z \mathbf{b}_W \mathbf{c}_W^2} &= - \int_0^1 dt \int_0^1 dx \int_0^\infty dz \frac{x^2 z}{(z+c_W^2)^2 (c_W^2 xt + \bar{x} + \beta z)} = -1.13281, \\
M_Z^2 \int \frac{d\chi d\chi_1 \tilde{\alpha}}{\mathbf{a} \mathbf{b}_e \mathbf{c} \mathbf{a}_W \mathbf{b}_Z \mathbf{c}_W^2} &= - \int_0^1 dt \int_0^1 dx \int_0^1 dy \int_0^\infty dz \frac{x^2 \bar{x} z^2}{(z+c_W^2)^2 (c_W^2 \bar{x}y + tx + \beta z)^2} = -0.807308, \\
M_Z^2 \int \frac{d\chi d\chi_1 \tilde{\beta}}{\mathbf{a} \mathbf{b}_e \mathbf{c} \mathbf{a}_W \mathbf{b}_Z \mathbf{c}_W^2} &= - \int_0^1 dt \int_0^1 dx \int_0^\infty dz \frac{x^2 z}{(z+c_W^2)^2 (c_W^2 \bar{x} + tx + \beta z)} = -1.06654, \\
M_Z^2 \int \frac{d\chi d\chi_1 \tilde{\gamma}}{\mathbf{a} \mathbf{b}_e \mathbf{c} \mathbf{a}_W \mathbf{b}_Z \mathbf{c}_W^2} &= - \int_0^1 dt \int_0^1 dx \int_0^\infty dz \frac{xz}{(z+c_W^2)^2 (c_W^2 \bar{x} + tx + \beta z)} = -1.39341, \\
M_Z^2 \int \frac{d\chi d\chi_1 \tilde{\delta}}{\mathbf{a} \mathbf{b}_e \mathbf{c} \mathbf{a}_W \mathbf{b}_Z \mathbf{c}_W^2} &= - \int_0^1 dt \int_0^1 dx \int_0^1 dy \int_0^\infty dz x \bar{x} \times \\
&\times \left(\frac{1}{2} \frac{z}{(z+c_W^2)^2 (c_W^2 \bar{x}y + tx + \beta z)} + x^2 \frac{z^2}{(z+c_W^2)^2 (c_W^2 \bar{x}y + tx + \beta z)^2} \right) = -0.779669,
\end{aligned}$$

where we use the following notations:

$$\begin{aligned}
a &= \bar{x}y + xz, & a_t &= \bar{x}y + xt, & \alpha &= x + \bar{x}y, & \alpha_t &= \bar{x} + xt, & \alpha_y &= \bar{x} + xy, \\
\alpha_2 &= cx + \bar{x}y, & \alpha_3 &= c_W^2 y \bar{x} + x, & \beta &= x \bar{x}, & \bar{x} &= 1 - x.
\end{aligned}$$

-
- [1] MOLLER, W. T. H. van Oers, AIP Conf. Proc. **1261**, 179 (2010).
[2] J. Benesch *et al.*, The MOLLER Collab., at http://hallaweb.jlab.org/12GeV/Moller/downloads/DOE_Proposal/DOE_Moller.pdf (2011). 2011
[3] J. Benesch *et al.*, www.jlab.org/~arnd/moller_proposal.pdf (2008);
[4] K. S. Kumar, AIP Conf. Proc. **1182**, 660 (2009).
[5] K. S. Kumar, E. Hughes, R. Holmes, and P. Souder, Mod.Phys.Lett. **A10**, 2979 (1995).
[6] K. Kumar, Eur.Phys.J. **A32**, 531 (2007).

- [7] SLAC E158 Collaboration, P. Anthony *et al.*, Phys.Rev.Lett. **92**, 181602 (2004), arXiv:hep-ex/0312035.
- [8] L. W. Mo and Y.-S. Tsai, Rev. Mod. Phys. **41**, 205 (1969).
- [9] L. Maximon, Rev.Mod.Phys. **41**, 193 (1969).
- [10] A. Czarnecki and W. J. Marciano, Phys. Rev. **D53**, 1066 (1996), arXiv:hep-ph/9507420.
- [11] A. Denner and S. Pozzorini, Eur. Phys. J. **C7**, 185 (1999), arXiv:hep-ph/9807446.
- [12] F. J. Petriello, Phys.Rev. **D67**, 033006 (2003), arXiv:hep-ph/0210259.
- [13] J. Erler and M. J. Ramsey-Musolf, Phys.Rev. **D72**, 073003 (2005), arXiv:hep-ph/0409169.
- [14] A. Aleksejevs, S. Barkanova, A. Ilyichev, and V. Zykunov, Phys. Rev. **D82**, 093013 (2010), arXiv:1008.3355.
- [15] A. Aleksejevs, S. Barkanova, A. Ilyichev, Y. Kolomensky, and V. Zykunov, (2010), arXiv:1010.4185.
- [16] A. Aleksejevs, S. Barkanova, Y. Kolomensky, E. Kuraev, and V. Zykunov, Phys. Rev. **D85**, 013007 (2012), arXiv:1110.1750.
- [17] C. Møller, Annalen der Physik **406**, 531 (1932).
- [18] V. Baier, V. Fadin, and V. Katkov, *Emission of relativistic electrons* (Atomizdat, Moscow, 1973).
- [19] A. Akhiezer and V. Berestetskij, *Quantum Electrodynamics*, 4 ed. (Nauka, Moscow, 1981).
- [20] T. Hahn, Comput.Phys.Commun. **140**, 418 (2001), arXiv:hep-ph/0012260.
- [21] T. Hahn and M. Perez-Victoria, Comput.Phys.Commun. **118**, 153 (1999), arXiv:hep-ph/9807565.
- [22] J. Vermaseren, (2000), arXiv:math-ph/0010025.
- [23] D. R. Yennie, S. C. Frautschi, and H. Suura, Ann. Phys. **13**, 379 (1961).
- [24] F. Bloch and A. Nordsieck, Phys. Rev. **52**, 54 (1937).
- [25] L. N. Lipatov, Sov. J. Nucl. Phys. **20**, 94 (1975), [Yad.Fiz.20:181-198,1974].
- [26] G. Altarelli and G. Parisi, Nucl. Phys. **B126**, 298 (1977).
- [27] E. A. Kuraev and V. S. Fadin, Sov. J. Nucl. Phys. **41**, 466 (1985).
- [28] E. Lifshitz and L. Pitaevskij, *Relativistic Quantum Theory*, Theoretical Physics Vol. 2, First ed. (Nauka, Moscow, 1971).